LBL-13072

Lawrence Berkeley Laboratory

UNIVERSITY OF CALIFORNIA

Materials & Molecular Research Division

RECEIVED
LAWRENCE
BERKELEY LABORATORY

OCT 21 1981

LIBRARY AND
DOCUMENTS SECTION

SURFACE STUDIES OF NICKEL

Cynthia Marie Friend
(Ph.D. thesis)

August 1981

TWO-WEEK LOAN COPY

This is a Library Circulating Copy which may be borrowed for two weeks. For a personal retention copy, call Tech. Info. Division, Ext. 6782

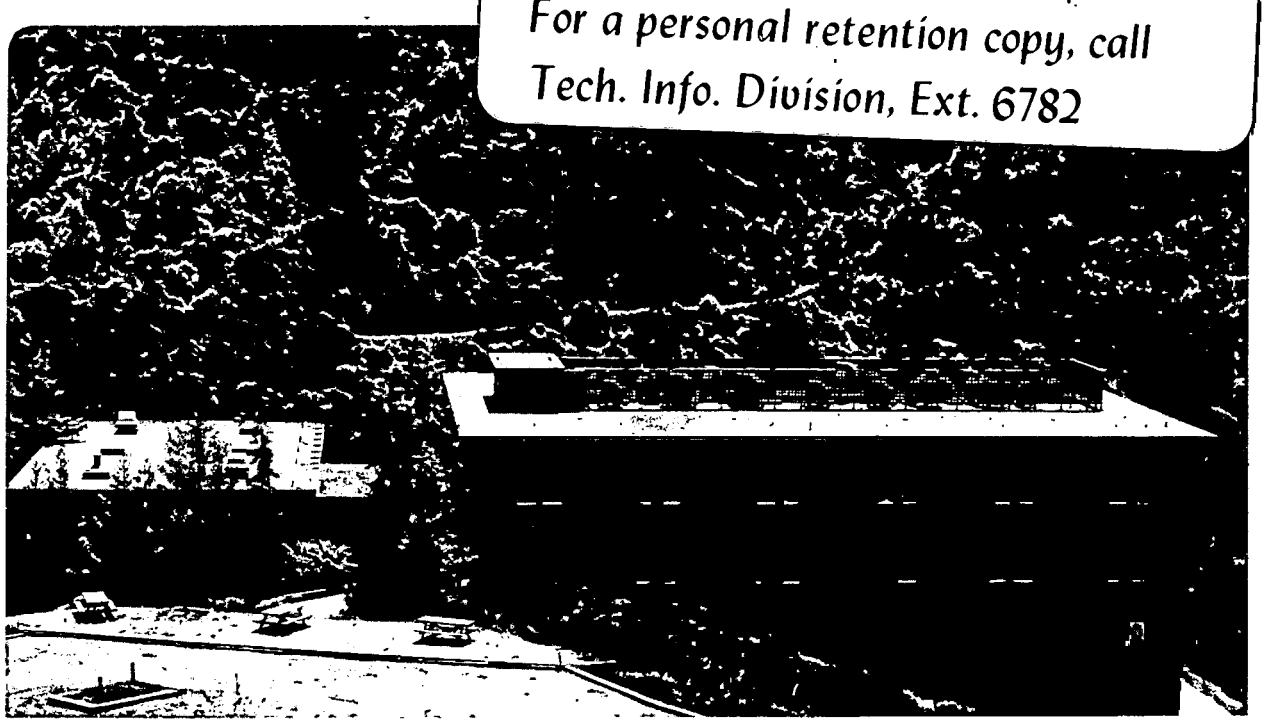

Prepared for the U.S. Department of Energy under Contract W-7405-ENG-48

DISCLAIMER

This document was prepared as an account of work sponsored by the United States Government. While this document is believed to contain correct information, neither the United States Government nor any agency thereof, nor the Regents of the University of California, nor any of their employees, makes any warranty, express or implied, or assumes any legal responsibility for the accuracy, completeness, or usefulness of any information, apparatus, product, or process disclosed, or represents that its use would not infringe privately owned rights. Reference herein to any specific commercial product, process, or service by its trade name, trademark, manufacturer, or otherwise, does not necessarily constitute or imply its endorsement, recommendation, or favoring by the United States Government or any agency thereof, or the Regents of the University of California. The views and opinions of authors expressed herein do not necessarily state or reflect those of the United States Government or any agency thereof or the Regents of the University of California.

LBL-13072

SURFACE STUDIES OF NICKEL

Cynthia Marie Friend
(Ph.D. Thesis)

Lawrence Berkeley Laboratory
and
University of California
Department of Chemistry
Berkeley, California 94720

This work was supported by the Director, Office of Energy Research, Office of Basic Energy Sciences, Chemical Sciences Division of the U. S. Department of Energy under Contract Number W-7405-ENG-48.

SURFACE STUDIES OF NICKEL

Cynthia Marie Friend

Materials and Molecular Research Division
Lawrence Berkeley Laboratory

and

Department of Chemistry
University of California
Berkeley, California 94720

ABSTRACT

The coordination chemistry of a range of molecules of catalytic importance adsorbed on nickel surfaces has been investigated. These studies have been performed as a function of surface crystallography and composition. Five crystallographic planes were utilized; the three low Miller index Ni (111), Ni(110) and Ni(100), the stepped Ni 9(111)x(111) and the stepped-kinked Ni 7(111)x(310) with carbon, sulfur and oxygen introduced as surface contaminants.

Detailed studies of the aromatic hydrocarbons, benzene and toluene, were performed. Thermal desorption spectroscopy and chemical displacement reactions were used in conjunction with isotope exchange reactions to delineate key factors that control C-H bond activation for these molecules adsorbed on nickel surfaces.

Reactive studies of the cyclic hydrocarbons, cyclohexane, cyclohexene, 1,3- and 1,4-cyclohexadiene, to form benzene were carried out using the same approach as for the arenes. Insight into the mechanistic details of the dehydrogenation reaction was gained on the basis of these experiments.

Additionally, the surface catalyzed isomerization of CH_3NC to form CH_3CN was observed on carbon or carbon and nitrogen contaminated nickel surfaces. The isomerization did not occur on clean nickel surfaces, thus

demonstrating a dramatic dependence of the chemistry on surface composition. Isotopic exchange reactions, chemical displacement, thermal desorption spectroscopy, complimentary catalytic reactions and high resolution electron energy loss spectroscopy were the techniques used to obtain structural, stereochemical and mechanistic information. Preliminary studies of chemisorbed pyridine, ethylene and acetylene are also described.

TABLE OF CONTENTS

I. Introduction 2

II. Experimental 15

III. Trimethylphosphine Chemisorption on Nickel Surfaces 24

IV. Arene Surface Coordination; Benzene and Toluene Chemisorption on Nickel Surfaces 32

V. Reactive Studies of C_6-cyclohydrocarbons on Nickel Surfaces .. 54

VI. Nickel Surface Chemistry of Methyl Isocyanide and Acetonitrile 62

VII. Appendix 113

VIII. Acknowledgements 117

IX. References 118

To My Parents

I. INTRODUCTION

The characterization of the chemistry and structure of catalytically important molecules adsorbed on metal surfaces is fundamental to the areas of surface science and catalysis. Through the understanding of the surface chemistry and physics associated with a range of molecules, key factors controlling catalytic reactions may be delineated.[1]

Nickel metal has been established as a catalyst for a broad range of heterogeneous reactions such as hydrogenolysis, hydrogenation and cyclization. For example, studies of substitution reactions of arenes have been performed using evaporated nickel films as catalysts[2]; the rate of HD exchange for equimolar amounts of C_6H_6 and C_6D_6 was rapid at 0°C. Additionally, supported nickel catalysts have been used for ethane hydrogenolysis with nickel being the most effective of the first row, group VIII metals for catalyzing this reaction.[3] In this thesis research, the surface chemistry of a range of hydrocarbons of catalytic interest adsorbed on nickel surfaces has been studied. These studies have been performed as a function of surface crystallography and composition. The five crystallographic planes, Ni(111), (100), (110), 9(111)x(111) and 7(111)x(310), shown in figures 1-3, were used in order to vary the surface topography and metal atom coordination number. In addition to the experiments performed on clean nickel surfaces, the effect of surface carbon, nitrogen, sulfur and oxygen on the chemistry were studied. In this way, factors that may be of key importance in catalytic reactions were studied in a systematic fashion.

The characterization of the chemisorptive properties of hydrocarbons is a particularly challenging problem. Due to the large number of atoms and structural variables, and the possibility of chemical reactions

Figure 1. Depicted in the figure are the three low Miller index planes of nickel. The (111) surface, on the upper left hand side is the close-packed, thermodynamically most stable with three-fold symmetry and a metal atom coordination number of 9. The (100) surface on the right has four-fold symmetry and surface metal atom coordination number of 8. The (110) or "super-stepped" surface shown on the bottom has a trough-like structure. The topmost atoms have a coordination number of 7 and the trough atoms, lying half a lattice constant below the plane have a coordination number of 11.

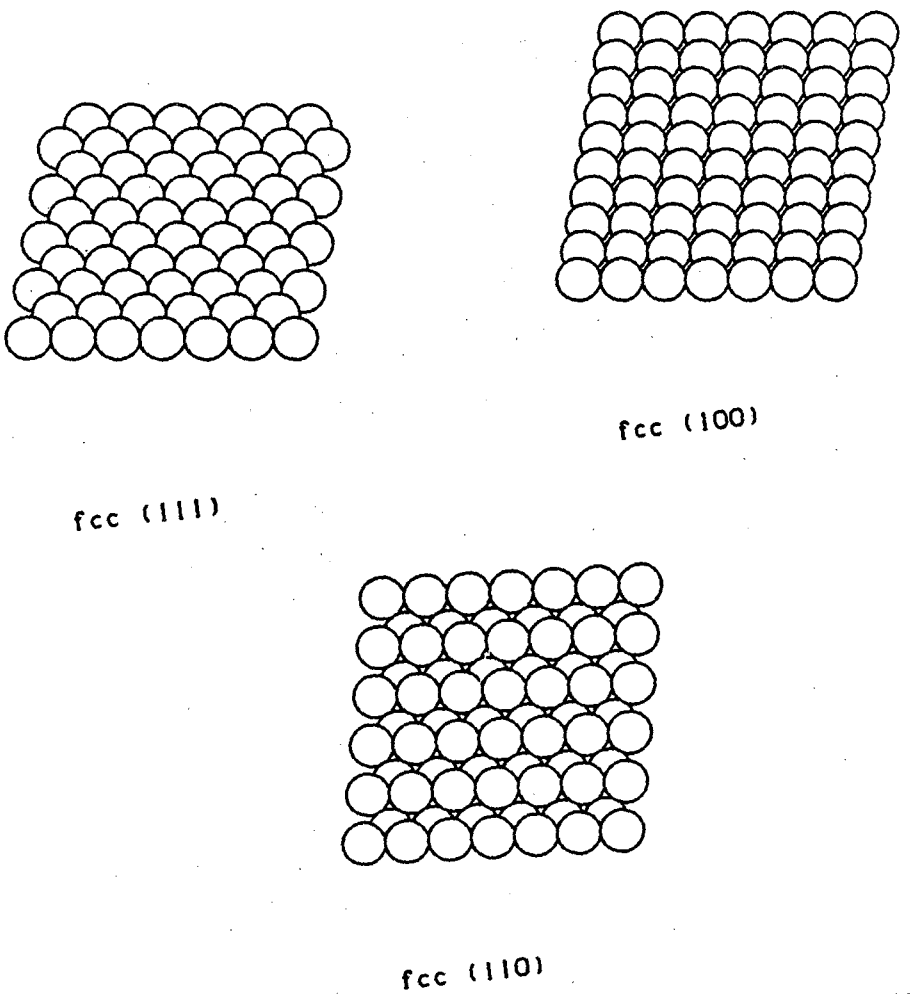

XBL 802-8036

Figure 1.

Figure 2. The stepped Ni 9(111)x(111) surface is alternatively indexed as Ni (997). The terraces illustrated with open circles are of (111) orientation and are nine atoms long in the (111) direction. The step atoms also are of (111) orientation but have a coordination number of 7 and are denoted by the lined circles.

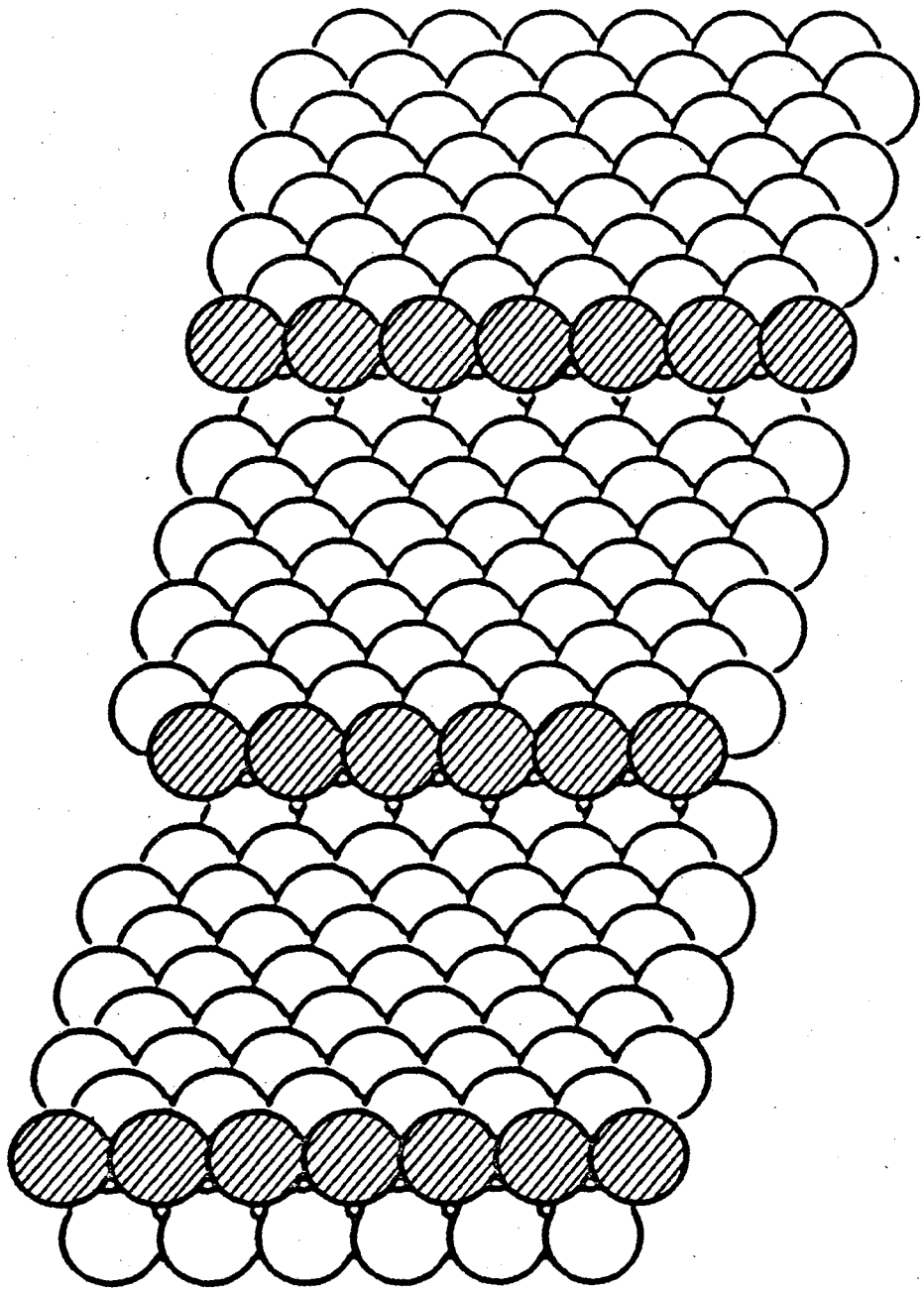

fcc 9(111)x(111)

XBL 802-8091A

Figure 2.

Figure 3. In this figure, the stepped-kinked Ni 7(111)x(310) surface is represented. The terraces, depicted by the open circles, are of (111) orientation and are 7 atoms long, the lined circles depict step atoms with a coordination number of 7 and the kink atoms denoted in black have a coordination number of 6. The alternative index for this surface is Ni(10,8,7).

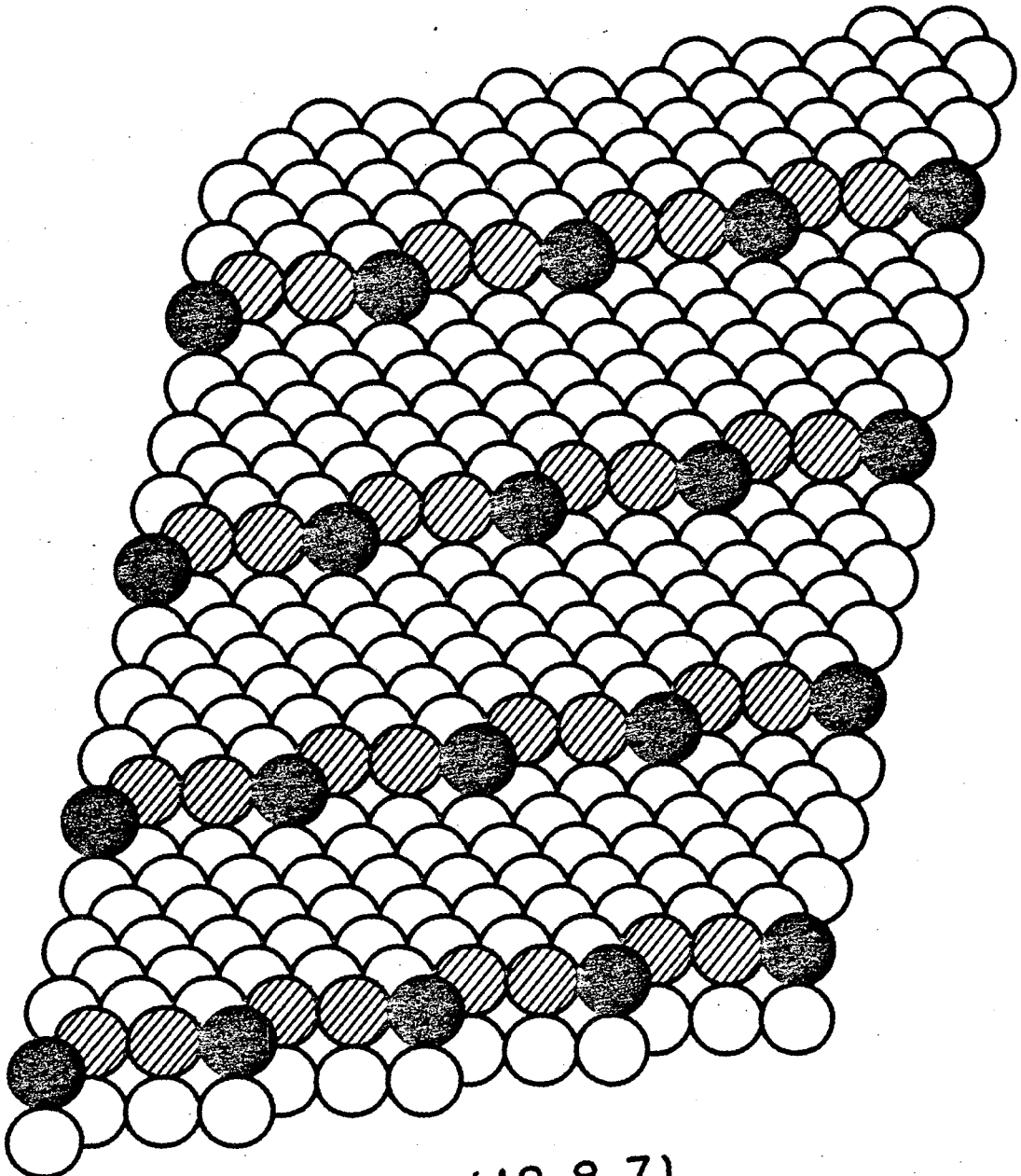

fcc (10,8,7)

XBL 802-8090A

Figure 3.

upon adsorption, there are innumerable models that may be considered for a given system. None of the conventional surface physics techniques such as low energy electron diffraction, ultra violet photoemission, or high resolution electron energy loss spectroscopy are amenable to unique interpretation of the data for these cases. The surface physical techniques are limited in that no adequate theoretical description is available to date. For example, multiple scattering events are significant in a low energy electron diffraction experiment. Thus, calculated intensity versus voltage (energy) data are only able to yield qualitative agreement with experimental results[4] often rendering one or more structural model plausible. Absolute orbital energies for adsorbed species may not be calculated for an ultraviolet photoemission spectrum. As a result, interpretations are usually based on a comparison of calculated and experimental energy splittings or comparison of orbital energy splittings of the gas phase and adsorbed molecule.[5] No clearcut selection rules have been established for high resolution electron energy loss spectroscopy because of the possibility of several different scattering mechanisms.[6] Thus, interpretation of surface vibrational data of relatively complex adsorbates is not straight-forward. For these reasons, a combined surface chemical and surface physics approach has been utilized in these studies in order to increase the amount of information available for interpretation. The surface chemistry that is observed yields information about the type of reactions that are occurring upon chemisorption and eliminate some general structural models. By considering the chemisorptive bond as a localized property, analogy can be made between organometallic cluster and surface chemistry.[7] There is a large base of information available for organometallic chemistry

which is subject to unambiguous interpretation. The chemical analogy places the interpretation of the surface studies in a chemically plausible context. The chemical techniques utilized in the surface studies are thermal desorption and chemical displacement reactions used in conjunction with isotopic labelling and catalytic reactions.

In a thermal desorption experiment, a molecule is adsorbed on the metal surface. The crystal is subsequently rapidly heated in an approximately linear fashion. The products thermally desorbed from the surface are monitored with a quadrupole mass spectrometer as a function of temperature and time. A simple kinetic model is used to describe the desorption process:[8]

$$\frac{-dN_i}{dt} = \nu_i \, N_i^{x_i} \, \exp\left(-E_i/RT\right) \qquad (1.)$$

where

N_i = population of the ith state (molecules/cm.^{2})

E_i = activation energy of desorption

ν_i = kinetic frequency factor

x_i = order of the desorption process.

In this formalism, an infinitely fast pumping speed is assumed, thus readsorption processes are neglected and the partial pressure of the ith species is directly proportional to the number of molecules desorbed from the surface. By optimizing equation (1.) with respect to the temperature and substituting for a linear heating rate, an expression for the desorption energy can be obtained in terms of the temperature where the maximum desorption rate occurs;

$$T_m = \frac{R}{E_i} \ln\left[\frac{dT/dt}{x_i \, \nu_i \, N_i^{x_i-1}} \; \frac{E_i}{R\,T_m^2}\right] \qquad (2.)$$

This equation can be solved iteratively for E_i, the desorption energy. The temperature where the maximum desorption rate occurs, T_m, and the heating rate, dT/dt, are measureable quantities. By varying the heating rate over a broad range, both the frequency factor and activation energy for desorption may be calculated. More commonly a typical vibrational frequency of 10^{13} sec.$^{-1}$ is assumed as the value of ν_i[8]. Such an assumed frequency factor may be off by several orders of magnitude as discussed in reference 9. This kinetic model assumes that ν_i and E_i are independent of the surface coverage. By varying the coverage, N_i, the order of the desorption, x_i, may be determined. For a first-order desorption (x_i=1), the temperature at which the maximum desorption rate occurs will be independent of coverage as $T_m \sim -\ln N_i^{x_i-1}$. For a second-order process (x_i=2), T_m decreases as a function of coverage. Physically, a second-order process is limited by the rate of recombination of the ith species on the surface. Thus, at low coverage the rate of encountering another molecule on the surface is lower at lower temperatures.

More generally the desorption experiment does not monitor a single reversible process. Several competing surface processes may be occurring as a function of temperature. Thermally induced decomposition or chemical reactions may occur before desorption. Desorption of a product of a thermally induced reaction may be studied to gain information about the activation energy of the reaction. There are two regimes for desorption of the product molecule, desorption limited and reaction limited. In a desorption limited process, the surface reaction occurs at a temperature lower than the desorption temperature, thus, the product will remain on the surface until thermal desorption can be effected. Invoking a simple kinetic model, an upper limit for the activation energy of reaction can be estimated. The precise temperature at which reaction

occurs cannot be identified by this technique. In the reaction limited case, the product is formed at a temperature higher than the normal desorption temperature. Thus, desorption occurs immediately following product formation. If again a simple kinetic model is assumed, an estimate for the activation energy of the reaction can be made.

The thermal desorption technique has some limitations in the application to the surface chemistry of reactive molecules such as hydrocarbons. Decomposition of the adsorbed species may be thermally induced during the course of the desorption experiment. In this case, the parent adsorbate is not desorbed quantitatively from the surface and cannot be studied in detail. Additionally, the temperature at which decomposition occurs may not be identified in the desorption limited case. A desorption method that does not thermally perturb the surface, namely chemical displacement, will allow for a more complete description of the surface structure and processes. The chemical displacement reaction is a formal analog to a ligand exchange or replacement reaction[10] in organometallic chemistry. In a chemical displacement reaction, the molecule of interest (A) is adsorbed on the metal surface at less than saturation coverage. This metal-adsorbate system is then exposed to a displacing molecule (B). In the simplest possible case, A will have adsorbed molecularly on the surface and will be quantitatively displaced from the surface by B without changing the surface temperature. Displacement is evidenced by detection of desorbed A in the gas phase by a quadrupole mass spectrometer. By performing a series of displacement reactions, a series of relative thermodynamic strength can be established for a variety of adsorbates.[11] Similarly, it may be possible to displace products of surface reactions. Schematically this may be repre-

sented as follows:

$$\underset{\sim}{A}_{(g)} \rightarrow \underset{\sim}{A}_{(ads)} \rightarrow \underset{\sim}{P}_{(ads)}$$

$$\underset{\sim}{P}_{(ads)} + \underset{\sim}{B}_{(g)} \rightarrow \underset{\sim}{P}_{(g)} + \underset{\sim}{B}_{(ads)}$$

The advantage of using the chemical displacement reaction is that the crystal temperature remains constant during the course of the experiment. Thus, the temperature dependence of surface reactions with displacable products can be studied in detail.

Alternatively, the adsorbed species (either $\underset{\sim}{A}$ or $\underset{\sim}{P}$) may not be completely desorbed from the surface during a displacement reaction. In the extreme case, no displacement of $\underset{\sim}{A}$ is observed for a range of displacing agents. Since the mechanism of the displacement reaction is unknown, no unambiguous conclusions may be drawn as both thermodynamic and kinetic factors may play a role. In some instances, partial displacement may be effected. In this case, it is important to attempt the reaction using a range of displacing gases as the extent of displacement may be dependent on the incoming adsorbate, $\underset{\sim}{B}$. An example of this behavior is benzene adsorbed on Ni(111).[6] Partial displacement over a large range of different displacing agents, is suggestive of multiple adsorption states, however, the results are inconclusive for the same reasons that negative displacement reactions are not subject to unambiguous interpretation. Care must be taken in interpreting negative displacement results.

Chemical displacement and thermal desorption techniques may be combined with isotopic labelling studies to further delineate the mechanistic details of surface reactions. For example, coadsorption of a mixture of perdeutero and perhydrido hydrocarbons followed by displace-

ment or thermal desorption may provide evidence for reversible or irreversible C-H bond scission in the desorbed species. The extent of displacement may be determined by performing a displacement reaction with the perdeuterohydrocarbon followed by thermal desorption. The amount of deuterium containing products produced in thermal desorption can be related to the extent of the displacement.

The major thrust of this work has been to delineate the key factors that control carbon-hydrogen bond cleavage processes in hydrocarbons adsorbed on nickel surfaces. This is an important issue to address as C-H bond scission is often invoked as the initial step in catalytic exchange and substitution reactions and is of key importance in dehydrogenation reactions. The techniques described above have been used to study the chemistry of a range of different hydrocarbons including arenes, olefins and paraffins. The chemical studies suggest that the predominant factor controlling C-H bond activation in hydrocarbons adsorbed on nickel surfaces is formation of a C-H-Ni bridging interaction in analogy to the coordination chemistry case.[13] In order for this type of interaction to occur, close approach of one or more hydorgen atoms to the nickel surface is required. Thus, surface topography and steric factors in the adsorbate both play important roles in the C-H bond cleavage process. The effect of surface impurities, namely, S, C and O were also studied.

Identification of novel catalytic reactions has also been a focus of this work. The surface chemistry of the isomeric molecules CH_3NC and CH_3CN has been studied on nickel surfaces. Via the ultra-high vacuum studies, the previously unreported metal catalyzed isomerization of CH_3NC to form CH_3CN was found to occur on nickel surfaces with carbon

and nitrogen or carbon impurities. The mechanism of the isomerization was established as fully intramolecular on the basis of isotopic labelling experiments. High resolution electron energy loss studies of these two isomers were performed on Ni(111) and Ni(111)-C surfaces. On the basis of the CN stretching frequency, both the CH_3CN and CH_3NC are proposed to reside in bridge sites on the clean surface. The observed ν(CN) for the two molecules was increased on the carbided surface with two different CN stretching frequencies observed for methyl isocyanide adsorbed on the carbided surface. This suggests that the carbide significantly changes the surface electronic properties. The role of the carbide in the isomerization reaction was not clearly defined.

II. EXPERIMENTAL

1. General Procedure and Reagents

Experiments were performed in a bakeable, ultra-high vacuum chamber (Varian) equipped with a ring of five 40 liter/sec. triode ion pumps and a titanium sublimation pump, with a working base pressure of $\simeq 2 \times 10^{-10}$ torr. A 99.999% purity single-crystal nickel rod (Materials for Research Corp.), $\sim$0.375 inches in diameter, was oriented to within 0.5° of the desired crystallographic plane using Laue X-ray back reflection. Spark erosion was used to cut a wafer such that the exposed surface was circular with approximately a 0.25 inch diameter and a circular ridge 0.3125 inches in diameter. The crystal was mechanically polished with four grades of alumina (the smallest particle size was $\simeq$10 microns), followed by 1 micron diamond paste and subsequently with 0.05μ alumina in water. Prior to being placed in the vacuum chamber, the crystal was chemically polished (etched) with a 3:1:1:5 mixture of the concentrated acids, HNO_3, H_2SO_4, H_3PO_4 and CH_3COOH[14] at a temperature of approximately 50°C, and subsequently rinsed with distilled water and ethanol. (The etching period must be brief, ca. 30 seconds in order to avoid pitting of the nickel surface).

The crystal was mechanically mounted on an x-y-z motion manipulator with a 2.5 inch offset and a 110° flip mechanism (Varian) by means of a tantalum cup that fit over the ridge. A button heater (Spectra Mat. Inc.), consisting of a tungsten filament imbedded in ceramic was mechanically held in place by the tantalum cup and used to indirectly heat the sample. The heating rate of the nickel crystal was 25°/sec. and was always linear in the range

of 50-400°C. New heaters were linear in the entire range of thermal desorption experiments. A liquid nitrogen cooled oxygen-free copper block was used to cool the crystal from 400°C to 25°C in approximately 5-10 minutes via mechanical contact with the crystal mount. Chromel-alumel thermocouple wires (.005 inches in diameter), spot welded to the crystal ridge, were used for temperature measurements.

The nickel crystal was cleaned in vacuum by a combination of ion sputtering and chemical techniques. Sulfur and phosphorous were removed by bombardment with 500 eV Ar^+ ions with a crystal temperature of approximately 600°C. Carbon and nitrogen were removed by treatment with 0.5-1.0 x 10^{-7} torr of O_2 for 1-2 minutes at a crystal temperature of ≈350°C. This was followed by treatment with 1.0-5.0 x 10^{-7} torr of H_2 for 5-10 minutes at ≈400°C. This procedure was repeated until the surface was clean. Surface cleanliness and composition were monitored using a four-grid, retarding field Auger electron spectrometer (Varian). Low energy electron diffraction was used to verify the crystallographic orientation of the surface and to identify any ordered overlayer structures. It is important to note that all of the surface phosphorous should be removed by Ar^+ ion sputtering prior to exposure to O_2. Treatment of a phosphorous contaminated nickel crystal with oxygen decreased the P(120 eV) Auger peak with a corresponding increase in the O(510 eV) Auger peak. Subsequent treatment with H_2 effected a decrease in the O(510 eV) peak with a concommitant increase in the P(120 eV) peak. The sputtering efficiency for phosphorous removal was much lower after treatment with oxygen as

compared to a nickel surface "freshly" contaminated with phosphorous. These data may be indicative of a Ni-P-O compound formation which caused penetration of P atoms below the surface nickel atoms.

Gas composition in the vacuum system was monitored with a quadrupole mass spectrometer (Uthe Technology International, model 100C) in conjunction with a commercial programmer (Uthe Technology International, PPSD) which externally drove the mass spectrometer and stored the ion current as a function of time. This allowed for scanning and storage of the integrated ion current for several different mass units in rapid succession (≈15 msec.). Using this configuration, the relative amounts of different isotopic species were compared upon exposure of the crystal and in thermal desorption or chemical displacement reactions. Thermal desorption was performed with the front face of the crystal directed along the line of sight of the mass spectrometer ionizer and isolated from the cooling block. Blank experiments, described later in this section, demonstrated that no detectable desorption from the cooling block occurred during the thermal desorption. The distance from the front face of the crystal to the mass spectrometer ionizer was approximately one inch. All thermal desorption experiments were performed without prior exposure of the crystal to an electron beam.

Gas exposures were performed with a variable leak valve equippped with a dosing "needle" such that the gases could be introduced in close proximity to the crystal surface, thus minimizing background contamination. Approximate gas exposures were determined by backfilling the vacuum chamber with a given gas to

a pressure of $\simeq 10^{-8}$ torr while monitoring the mass spectrometer parent ion current, yielding a pressure versus ion current correlation. During all gas exposures, the parent ion current was monitored as a function of time and later integrated over time to yield an approximate exposure in terms of Langmuirs (1 Langmuir = 1 L. = 10^{-6} torr-sec.). The total pressure in the vacuum chamber during gas exposures was always maintained at $\lesssim 1 \times 10^{-8}$ torr.

Two separate valve-needle assemblies mounted symetrically with respect to the mass spectrometer were used to introduce the different gases in a chemical displacement reaction. The two inlets were necessary to avoid any cross-contamination of the different gases within the valves. Blank experiments demonstrated that there was no cross-contamination within the valves or manifold. After initial exposure of the crystal to gas $\underset{\sim}{A}$. the sample was rotated to face the second valve assembly. The displacing gas, $\underset{\sim}{B}$, was then introduced while monitoring the integrated ion current for gases $\underset{\sim}{A}$, $\underset{\sim}{B}$ and other possible products of the displacement reaction. If displacement occurred, a peak in the $\underset{\sim}{A}^+$ ion current was detected. Given that the crystal was directed 45° away from the line of sight of the mass spectrometer ionizer, the intensity of the signal for the displacement products was reduced significantly in comparison with a line of sight measurement. This observation is consistent with a distribution of desorbing particles peaked in a direction perpendicular to the crystal surface. The time interval between initial exposure of $\underset{\sim}{A}$ and exposure by the displacing agent, $\underset{\sim}{B}$, was approximately three minutes in all cases.

Blank experiments were performed in order to verify that the chemistry observed was associated with the exposed nickel surface.

A wafer of single-crystal nickel was cut as described above. The wafer was soft soldered onto a copper disk (0.06 inches thick, 0.75 inches diameter), with a copper wire attached for handling. A rubber mask was applied to the side and edges of the nickel crystal such that only the 0.25 inch diameter surface was exposed. The masking procedure was repeated three times at eight hour intervals. The sample was prepared for plating in a series of steps, with rinsing with distilled water between each step. Trichloroethylene was used as a degreaser, followed by treatment with a caustic cleaner and hydrochloric acid. The surface was activated by a nickel chloride-hydrochloric acid strike (electrodeposition of a very thin layer of nickel metal), followed by a copper strike. The exposed face was then gold plated using a low cyanide concentration, commercial process (Technic Hg Gold Process). The final thickness of the gold layer was 2×10^{-4} inches. Following the plating, the rubber mask was peeled away and the crystal removed from the copper disk. Excess solder on the back of the nickel crystal was mechanically removed with silicon carbide paper. The sample was then chemically polished (etched) and rinsed with H_2O and ethanol for all nickel crystals (see above). The gold surface appeared homogeneous with no visible sign of nickel. In fact, no nickel was detected when the crystal was examined in the vacuum chamber by Auger electron spectroscopy. The gold plated blank crystal was cleaned in the vacuum chamber by the O_2 and H_2 treatment described above for the cleaning of the nickel surface.

Low energy electron diffraction was used to check the orienta-

tion and surface ordering of the clean metal and to determine the unit cell of ordered overlayer structures of adsorbates or impurity atoms.

Reagent grade benzene and toluene were stored over CaH_2 and used without further purification. The perdeutero reagents (Aldrich Chemical Co. 99.9% ^{+}d) were handled similarly. The partially labelled toluenes, $CD_3C_6H_5$ and $CH_3C_6D_5$, were obtained from Merck and Co. and used without treatment. Trimethylphosphine and perdeutero-trimethylphosphine were synthesized by a modification of a literature preparation.[15] Acetonitrile was commercially obtained (Mallinckrodt Chemical Co., Research purity) dried over CaH_2 and used without further purification. CD_3CN (99.9% ^{+}d) and $CH_3C^{15}N$ (99% ^{15}N) were purchased from Aldrich Chemical Co. and Stohler Isotope Chemicals, respectively.

Methyl isocyanide was prepared[17] by the method of Cassanova and coworkers.[16] The material was stored under vacuum at -78°C following synthesis.

CD_3I was purchased from Aldrich Chemical Co. in a sealed ampule and used without further purification. KCN and $AgNO_3$ were obtained from Mallinckrodt Chemicals. AgCN was prepared by reaction of equimolar amounts of KCN and $AgNO_3$ in aqueous solution. D_2O was purchased from Biorad.

Methyl-d_3-isocyanide was prepared[17] by a modification of the method of Gautier.[18] A 100 ml. side-arm, single-neck flask equipped with a stir bar and a water-cooled reflux condensor was charged with 8.0 g (0.6 moles) of AgCN and 8.7 g. (0.6 moles, 3.9 ml.) of CD_3I. The flask was purged with argon and heated in a

steam bath for 4 hours during which time either a brown liquid or gummy solid formed. Stirring was interrupted and the flask allowed to cool to room temperature. A saturated solution of KCN in D_2O was then added with stirring. Stirring was continued for 1/2 hour and a brown liquid layer above the water became apparent. Impure methyl d_3-isocyanide (largely contaminated with methyl iodide) was collected by vapor transfer of the volatile material into a storage flask equipped with a Kontes high vacuum stopcock. The methyl-d_3-isocyanide was purified by preparative scale gas chromatography by using a 50 ft. 20% Carbowax 20M on Chromosorb W column at 60°C. The purity of the sample was established by mass spectral analysis and by gas chromatography (99.7%).

Methyl iodide, purchased from Mallinckrodt Chemical, was purified by distillation and stored in dark bottle over a bead of mercury. $K^{13}CN$ (56% isotopically labelled) was purchased from Isomet Co. $Ag^{13}CN$ (56% labelled) was prepared by reaction of equimolar amounts of $K^{13}CN$ and $AgNO_3$ in aqueous solution.

Methyl isocyanide-^{13}C was prepared[17] and purified in a manner analogous to that of methyl-d_3-isocyanide. Mass spectral analysis indicated that the sample purity was greater than 99.8% methyl isocyanide of which 56% was $CH_3N^{13}C$.

Cyclohexane and d_{12}-cyclohexane were obtained commercially, dried over Na_2SO_4 and used without further purification. Cyclohexene (Chem Samples Co., 99.9% purity) and d_{10}-cyclohexene (Merck Isotopes, 99%-d) were dried over CaH_2 and used without further purification. 1,3- and 1,4-cyclohexadiene were commercially obtained and their vapor stored in a high vacuum flask at 0°C. All reagents were checked for purity by mass spectral analysis.

2. High Resolution Electron Energy Loss Studies

This section of the experimental describes the details of the high resolution electron energy loss studies performed on CH_3CN and CH_3NC adsorbed on Ni(111) and Ni(111)-C surfaces at General Motors Research Laboratories.

All experiments were performed in a bakeable, all metal ultra high vacuum chamber with a working base pressure of 10^{-10} torr. The vacuum system was equipped with low energy electron diffraction optics, an Auger electron spectrometer, a high resolution electron energy loss spectrometer, a multiplexed quadrupole mass spectrometer and a liquid nitrogen cooled manipulator, all described in detail elsewhere.[19]

A 9 mm. diameter single-crystal nickel rod (99.999% purity, Materials for Research Corporation) was oriented to within 0.5° of the (111) direction using Laue X-ray back reflection techniques. A wafer (0.1 inches thick) was cut using spark erosion and polished as described in the General Procedure and Reagents section of this thesis. The crystal wafer was mounted on two 0.20 inch diameter nickel wires spot-welded to the back of the crystal and to tantalum supports on the manipulator. Chromel-alumel thermocouple wires spot-welded to the edge of the crystal were used for temperature measurement. The crystal was cleaned in vacuum by the same method described in the previous experimental section herein.

The gas exposures were performed at a crystal temperature of 100 K (-170°C) with the front face of the crystal directly in front of a multi-channel doser array. Using this configuration, the base pressure of the vacuum system remained below 1×10^{-9} torr

during gas exposures. Equivalent exposures in terms of Langmuirs (1 L= 10^{-6} torr-sec.) were estimated by comparing thermal desorption profiles from background exposures. One Langmuir (1.0 L) equals 3.2 x 10^{14} molecules/cm.^{2} for CH_3CN and CH_3NC assuming a gas temperature of 25°C.

During thermal desorption experiments, the adsorbed gas was desorbed directly into the mass spectrometer ionizer. The crystal was resistively heated through the nickel support wires with an approximately linear rate of 7-10°C/sec. The mass spectrometer was multiplexed so that several different mass units could be monitored in rapid succession during thermal desorption experiments.

The Ni(111)-C surface was prepared by thermally decomposing ethylene on the nickel surface at 300°C. Auger electron spectroscopy was used to confirm that the carbon on the surface was caribidic. The carbide surface was ordered, yielding a diffraction pattern similar to that reported by Bertolini and Tardy.[20] No energy losses associated with a Ni-C vibration could be observed on the carbided nickel surface.

The incident beam energy for the high resolution electron energy loss studies was approximately 2 eV with a full width at half maximum of 10 meV for the elastically scattered beam.

III. TRIMETHYLPHOSPHINE CHEMISORPTION ON NICKEL SURFACES

Trimethylphosphine is a widely used ligand in transition metal coordination compounds. It has been shown to be a strong, effective displacing ligand, readily replacing CO and arenes in organometallic compounds.[10] In this work, the thermal decomposition behavior of $P(CH_3)_3$ has been investigated and the phosphine successfully used as a displacement agent for a range of different adsorbates on nickel surfaces. The molecular details of trimethylphosphine chemisorption have not been fully studied because this research has been focused on hydrocarbon chemistry; the utility of the phosphine in this work has been as a displacing agent. Nevertheless, some plausible models for the chemisorption of the phosphine are suggested in analogy to existing organometallic compounds and are discussed herein.

Results and Discussion

Trimethylphosphine readily adsorbed with a sticking coefficient near unity on all nickel surfaces studied; the three low-Miller index planes, the stepped 9(111)x(111) and the kinked 7(111)x(310) depicted schematically in Figures 1-3. The thermal desorption behavior of trimethylphosphine adsorbed at 25°C was qualitatively the same for all five nickel surfaces. No thermally induced desorption of intact $P(CH_3)_3$ or other phosphorous containing species such as $HP(CH_3)_2$ and PH_3 was detected. The decomposition products, CH_4 and H_2, were thermally desorbed with carbon and phosphorous remaining on the surface. The specific desorption maxima for the five nickel surfaces studied are summarized in Table 1. Thermal decomposition following coadsorption of deuterium atoms and $P(CH_3)_3$ at 25°C yielded significant quantities of CH_3D and HD

TABLE 1

DECOMPOSITION OF $P(CH_3)_3$ ON FIVE NICKEL SURFACES

Surface	$T_m^{CH_4}$(°C)	$T_m^{H_2}$(°C)	$T_m^{H_2}$(°C)**
Ni(111)	90	100	120
Ni(100)	117,134*	102,174*	70
Ni(110)	100	170	-
Ni 9(111)x(111)	90	100	120
Ni 7(111)x(310)	90	100	120

* Unresolved double maximum.

**Thermal desorption maximum observed for adsorption of molecular hydrogen at saturation coverage.

and a trace amount of CH_2D_2 in addition to CH_4 and H_2. The temperatures at which the rate of desorption of the decomposition products is significant are lower than the temperatures at which D_2 itself desorbs from the clean surface. (See Table 1). Thus, the thermal decomposition of $P(CH_3)_3$ can be used as a means of detecting free deuterium atoms on the nickel surface at lower temperatures then would be possible without the phosphine decomposition. This is helpful in identifying significant C-D bond cleavage processes for a range of different hydrocarbons. (See later chapters for a more detailed discussion.)

The low temperature at which thermal desorption of the decomposition products of $P(CH_3)_3$ occurs is suggestive of dissociative adsorption on nickel. Either carbon-hydrogen or phosphorous-carbon bonds or both may be cleaved upon interaction with the metal surface. An example of a coordination compound in which a methyl hydrogen atom has been abstracted to yield hydride and $-P(CH_3)_2(CH_2)-$ coordinated to the Fe metal center is shown in Figure 4.[21] An analogous configuration is possible for trimethylphosphine adsorbed on nickel surfaces. Alternatively, abstraction of a methyl radical to yield chemisorbed CH_3 and $P(CH_3)_2$ is a possibility although there is no coordination chemistry analog for this model. Cleavage of one or more C-H bonds in $P(CH_3)_3$ must be effected at relatively low temperatures based on the thermal desorption maximum for H_2 following adsorption of the phosphine. The incorporation of surface deuterium atoms into the decomposition products is clear evidence of a decomposition mechanism involving surface recombination with hydrogen atoms. It is not necessary to invoke an adsorbed

Figure 4. Shown here is an iron coordination compound where there has been an internal oxidative addition of a C-H bond so as to yield a hydride and a CH_2 group that bridges both phosphorous and Fe. This is one possible model for $P(CH_3)_3$ coordination to the Ni surfaces at or near room temperature.

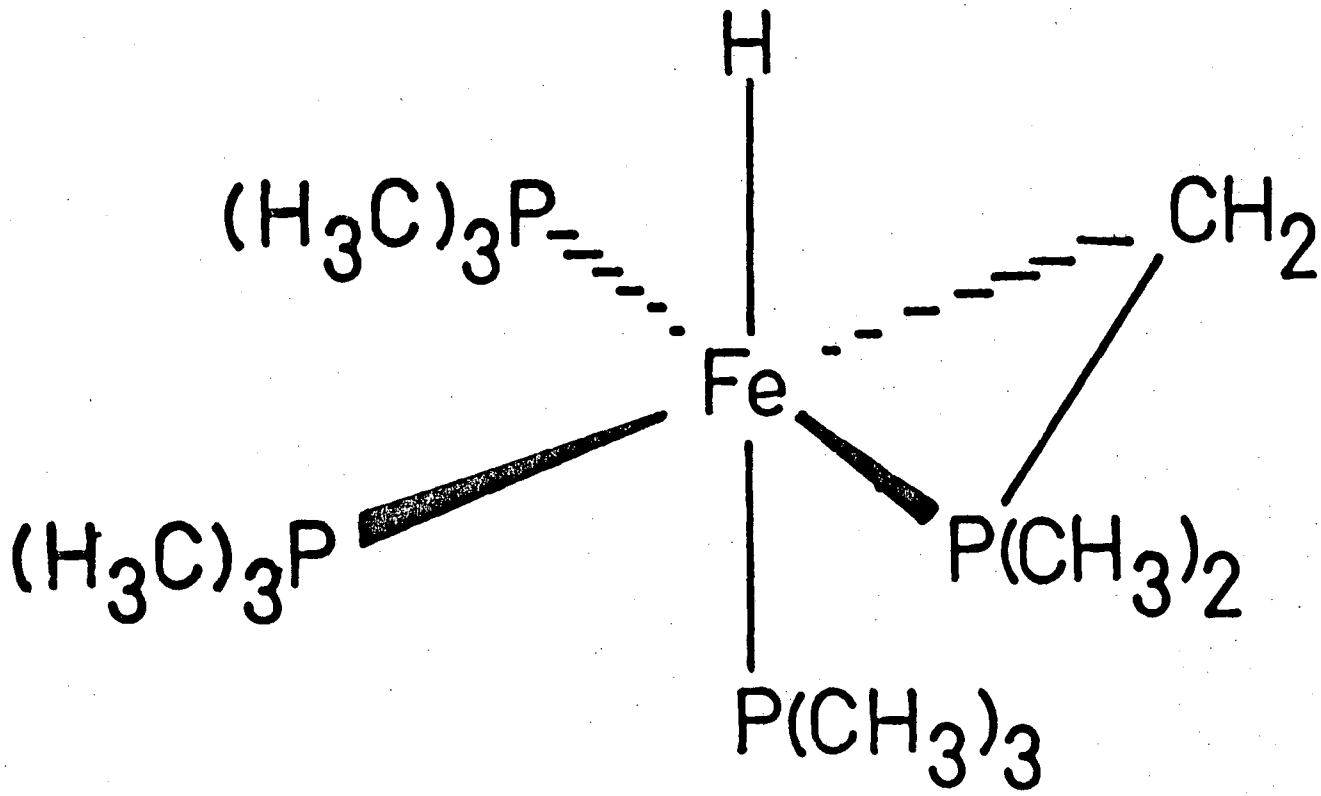

Figure 4.

XBL 815-9479

methyl radical species to account for methane formation as it may be possible to attack the P-CH_3 bond with surface hydrogen atoms to directly yield gaseous methane. The absence of a significant fraction of CH_2D_2 and CHD_3 molecules suggests that direct attack of the phosphorous-carbon bond of a P-CH_2 or P-CH function or surface recombination of CH_2 or CH species with hydrogen atoms is a minor reaction at best. Many other models may be proposed; in order to distinguish among them, more detailed spectroscopic studies (e.g. high resolution electron energy loss or ultraviolet photoemission spectroscopies) of the surface species must be performed in order to more clearly define the adsorption behavior of the phosphine. The low desorption temperature of H_2 from the phosphorous contaminated nickel surfaces suggests a dramatic modification of the surface electronic properties induced by the phosphorous. This effect is not understood at this time but may be studied by using ultraviolet photoemmission and work function change measurements.

Trimethylphosphine is of primary interest because of its role as a displacing agent. $P(CH_3)_3$ has been used to displace a range of different ligands in organometallic coordination compounds.[30] In this work, $P(CH_3)_3$ has also been found to be an effective displacing gas for a range of different adsorbates on nickel surfaces. Trimethylphosphine readily displaces benzene, CO and CH_3CN from the nickel surfaces studied at 25°C. In contrast, no displacement of other adsorbates, such as toluene, CH_3NC, ethylene and acetylene was detected. These results cannot be strictly interpretted in terms of structure or thermodynamics in analogy to the coordination chemistry case. The mechanism

of surface displacement by $P(CH_3)_3$ is not understood, thus the reaction can only be interpreted when desorption is effected.

Conclusion

Trimethylphosphine has been shown to be an effective displacing agent which can be used as an isothermal probe of some reactions on nickel surfaces. The mechanism of the displacement has not been investigated so that negative displacement reactions are not subject to unambiguous interpretation. The thermal decomposition behavior of the phosphine is suggestive of dissociation of one or more hydrogen atoms and possibly methyl radical upon adsorption of $P(CH_3)_3$ on the nickel surfaces studied. The structural details may be more fully characterized using surface spectroscopic techniques such as high resolution electron energy loss spectroscopy or uv photoemmission.

Phosphorous impurities on the nickel surface significantly alter the desorption energy of H_2 from the surface. A qualitative change in the chemistry associated with the Ni-P surface in comparison to the clean nickel surface is suggested by these results.[16] This is an area that warrants further investigation.

IV. ARENE SURFACE COORDINATION CHEMISTRY: BENZENE AND TOLUENE CHEMISORPTION ON NICKEL SURFACES

Nickel metal is an important catalyst for the hydrogenation of aromatic hydrocarbons.[23] In order to understand the mechanism of arene hydrogenation, the chemisorptive properties of the surface reactants must be delineated. Specifically, identification of significant C-H bond cleavage processes is important, as it may yield indirect structural information and may be suggestive of reaction intermediates for the catalytic hydrogenation reaction.

In this work, surface chemical studies have been employed to study the adsorption of benzene and toluene and to identify C-H bond breaking reactions on nickel surfaces at temperatures greater than ∿20°C. The chemisorption of benzene and toluene was investigated on five crystallographic planes (Figures 1-3) in order to study the effect of surface topography. Additionally, carbon, sulfur and oxygen atoms were selectively introduced as surface impurities to determine if these adatoms influenced the chemistry of benzene and toluene on nickel surfaces. These studies assisted the identification of potentially important factors in the catalytic hydrogenation of arenes in "real world" systems.

1. Results and Discussion

The chemistry of benzene and toluene has been studied on five different crystallographic planes (Figures 1-3) in order to determine the effects of geometry and of lower metal atom coordination number. The chemistry associated with the flat Ni(111) surface will be described in detail and compared with the results obtained on the other crystallographic planes.

Benzene adsorbed on a Ni(111) surface forms an ordered

structure yielding a $2\sqrt{3}x2\sqrt{3}/R30°$ diffraction pattern. Thermal desorption of C_6H_6 or C_6D_6 adsorbed on Ni(111) at ∿25°C yielded a small amount (∿10%) of intact benzene with a desorption maximum of approximately 115-125°C. The remaining benzene thermally decomposed on the surface producing H_2 or D_2 with a desorption maximum of ∿150°C and a carbon overlayer. Thermal desorption of a mixture of C_6H_6 and C_6D_6 adsorbed at room temperature yielded no isotopically mixed species (e.g. $C_6D_xH_{6-x}$) in the thermally reversible benzene fraction. Similarly, coadsorption of deuterium and C_6H_6 on the Ni(111) surface yielded no detectable H-D exchange products. These data clearly show that no detectable reversible C-H bond cleavage occurs at room temperature in that fraction of the benzene that was thermally desorbed.

Chemical displacement reactions were used to define the chemisorptive behavior of the thermally irreversible fraction of benzene. Trimethylphosphine quantitatively displaced benzene from Ni(111) at 25°C. This was evidenced by the detection of a peak in the benzene parent ion vs. time spectrum upon exposure of the benzene-Ni(111) crystal to $P(CH_3)_3$. A typical chemical displacement profile is shown in Figure 5. The thermal desorption spectrum following displacement of C_6D_6 by $P(CH_3)_3$ showed that no deuterated species were produced during decomposition (i.e. HD, D_2 or CH_3D) and no benzene. Analogous experiments with an adsorbed C_6H_6-C_6D_6 mixture yielded no detectable isotopically mixed benzene in the chemical displacement reaction and no HD, D_2 or CH_3D upon subsequent thermal decomposition. Irreversible C-D bond breakage could be achieved by adsorbing benzene at temperatures $\gtrsim$100°C. Perdeutero-benzene initially adsorbed near 100°C

Figure 5. The spectrum obtained from a displacement reaction of C_6D_6 from Ni(111) at 25°C by trimethylphosphine is shown in the figure. The top trace is the mass 61 ion current vs. time profile corresponding to the $P(CH_3)_3$ exposure. Mass 84, corresponding to $C_6D_6^+$ parent ion, is shown on the bottom. The peak in the 84 amu profile is attributed to C_6D_6 displaced from the surface.

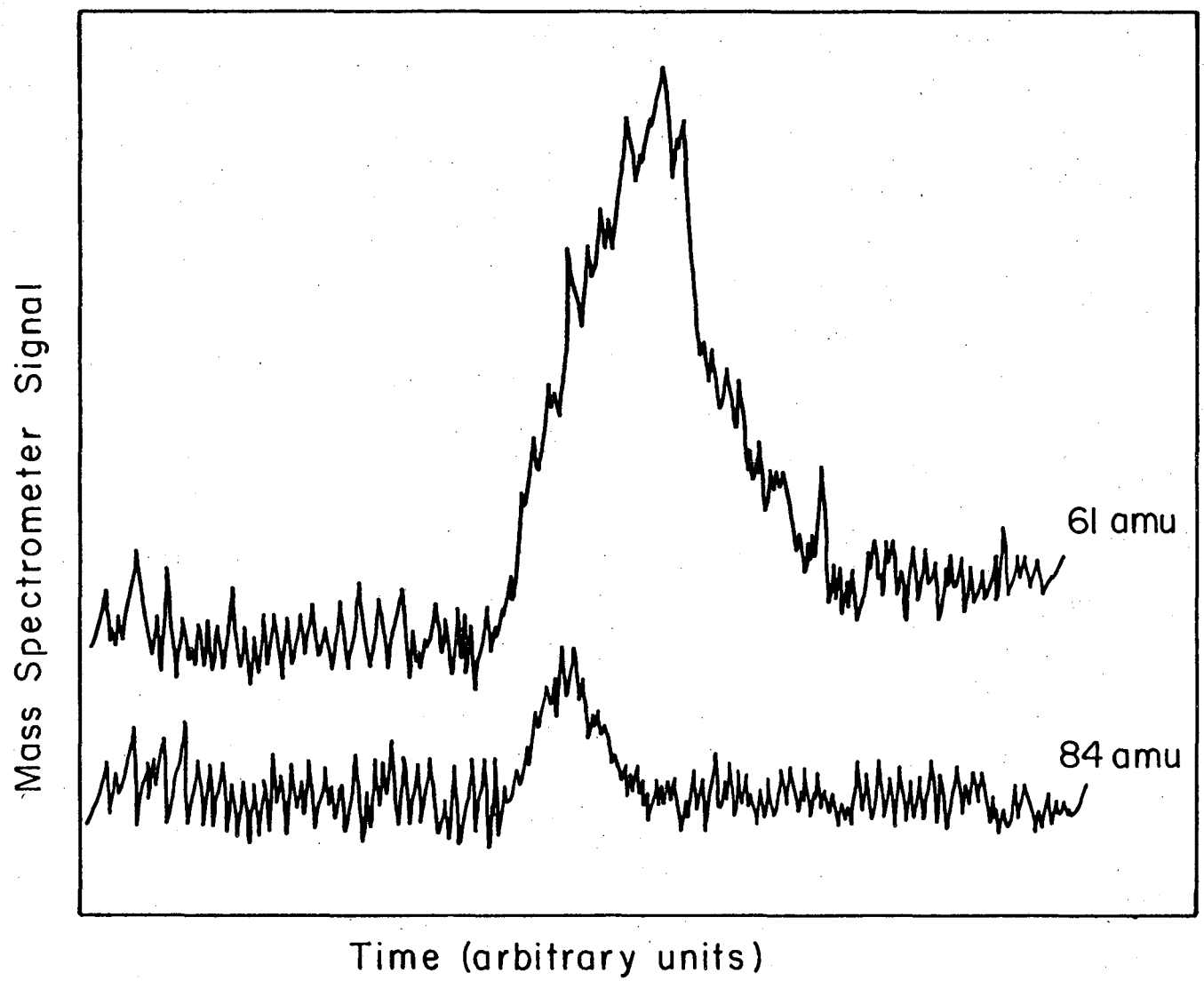

Figure 5.

XBL 806-5307

could not be displaced by trimethylphosphine at room temperature. In addition, copious amounts of HD and CH_3D were produced in the subsequent thermal decomposition reaction. This demonstrated that the decomposition behavior of trimethylphosphine was not altered by the presence of decomposed benzene on the surface, and thus was a good indicator of C-D bond cleavage. Additionally, these experiments identified the approximate temperature at which irreversible C-H bond scission is significant for benzene chemisorbed on Ni(111). Qualitatively similar results were obtained in experiments where CH_3NC was used as the displacing agent. Methyl isocyanide was not as effective as trimethylphosphine, as only partial displacement of benzene could be effected.[24]

No background desorption of benzene was detected from chemical displacement and thermal desorption experiments performed on a Au-plated blank. (Some $P(CH_3)_3$ reversibly adsorbed on the gold surface, but this was not relevant to the results obtained on nickel.) Thus, the chemistry observed must be attributed to the Ni(111) surface.

All the data obtained clearly indicate that benzene is molecularly bound to the Ni(111) surface at room temperature. No reversible or irreversible C-H bond cleavage is operative below temperatures of $\simeq 100°C$. The surface chemistry of benzene on Ni(111) is consistent with a structure proposed on the basis of high resolution electron energy loss[25,26] and ultraviolet photoemmission[27] studies. In this model, benzene is coordinated to the nickel surface in a π-fashion with the plane of the aromatic ring essentially parallel to the surface plane. (Figure 6.) The absence of C-H bond breaking rigorously excludes a σ-bound phenyl

Figure 6. Depicted here is the proposed model for benzene chemisorbed on flat nickel surfaces. The plane of the C_6-ring is essentially parallel to the metal surface with bonding occurring through an interaction of the π and π^* orbitals of benzene with metal surface orbitals.

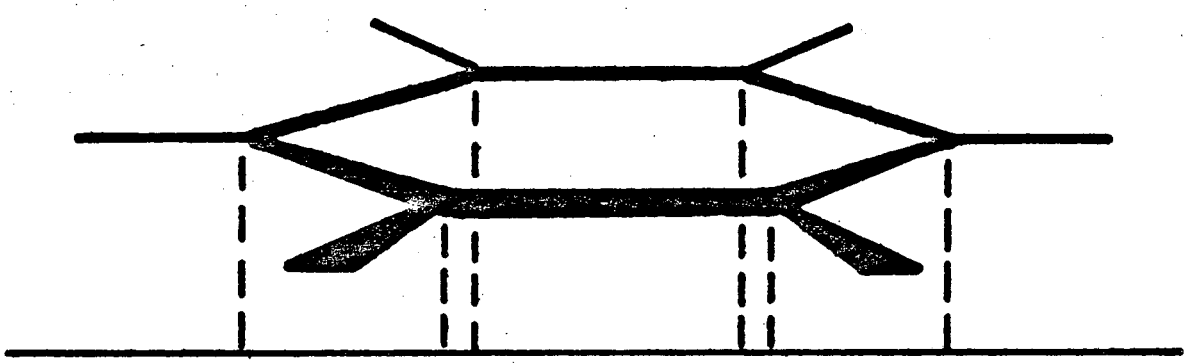

Figure 6. XBL 804-9452

radical.

Benzene chemisorption was studied on the stepped Ni 9(111)x(111) and stepped-kinked Ni 7(111)x(310). (Figures 2,3.) These surfaces consist mainly of flat (111) terraces, the width of which is large enough to accomodate a benzene coordinated parallel to the terraces. The step and kink atoms are of lower coordination number and introduce topographical irregularities in the flat surface. These experiments defined the role of surface irregularities in benzene chemisorption by comparison to the (111) case.

The thermal desorption data obtained on both the stepped and stepped-kinked surfaces were essentially identical to that of Ni(111) under similar conditions. Chemical displacement of perdeutero-benzene by trimethylphosphine from Ni 9(111)x(111) and Ni 7(111)x (310) was readily effected at room temperature. The thermal decomposition profile obtained following the displacement reaction contained small, but significant amounts of HD and CH_3D, in contrast to the Ni(111) case. Displacement of a mixture of C_6H_6 and C_6D_6 yielded no detectable isotopically mixed products. The residual deuterium on the stepped and stepped-kinked surfaces is clear evidence of C-H bond scission at temperatures <90°C. This relatively facile C-H bond cleavage must be attributed to the presence of step and kink atoms. One possible structure that accounts for this behavior is shown in Figure 7. In this model, the benzene ring π-coordinates to the (111) terrace allowing for interaction of one or more of the aromatic hydrogen atoms with nickel atoms of lower coordination number (i.e. step or kink atoms). As a result of this additional C-H-Ni interaction at step or kink sites, benzene is more strongly bound and C-H bond cleavage is facilitated.

Figure 7. Shown here is one possible model for benzene adsorbed on stepped or stepped-kinked nickel surfaces. In this model, the benzene ring is coordinated in a π-fashion to the flat Ni(111) terraces. This may allow for interaction of one or more of the aromatic hydrogen atoms with step or kink sites forming a C-H-Ni bridging interaction. Thus, CH bond cleavage would be facilitated via these interactions, consistent with the significant degree of CH bond cleavage observed experimentally.

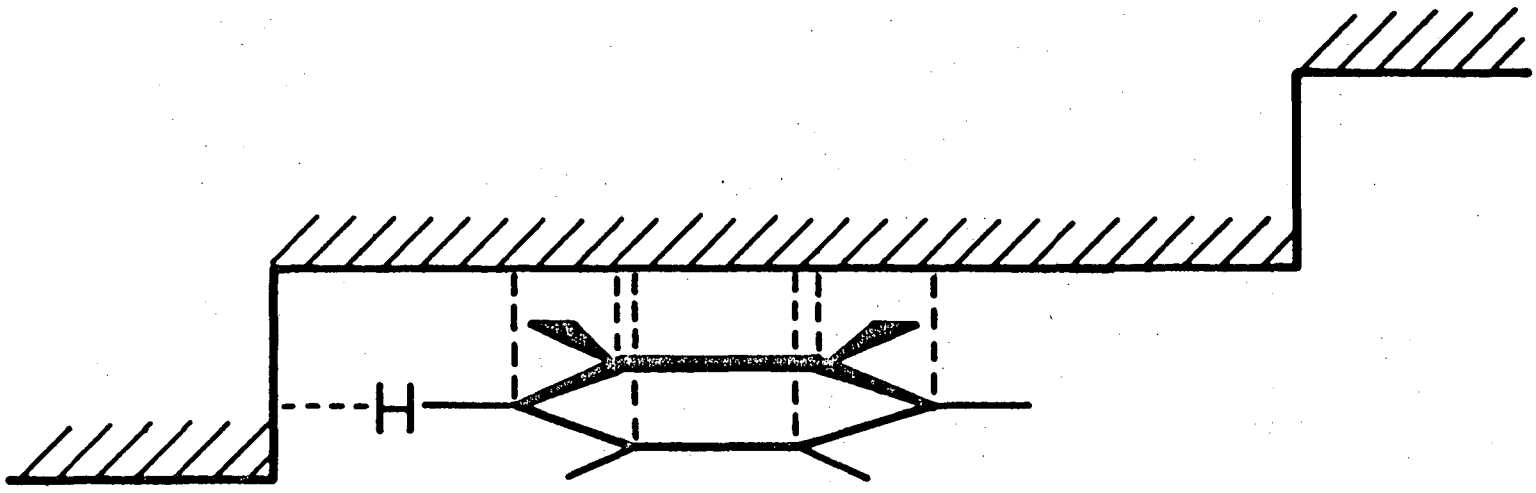

XBL 817-10649

Figure 7.

Chemisorption of benzene on the low Miller index Ni(100) and Ni(110) planes was also studied. Benzene-Ni(100) yielded a c(4x4) diffraction pattern at room temperature.[26] In contrast, no ordered diffraction pattern was observed for benzene adsorbed on Ni(110) under similar conditions. In both cases, benzene adsorbed at ≈25°C was partially thermally desorbed with desorption maxima occurring at ≈100°C and ≈230°C for Ni(110) and Ni(100), respectively. Chemical displacement of C_6D_6 by trimethylphosphine was effected at room temperature. Trace amounts of deuterium-containing decomposition products (CH_3D and HD) were detected upon subsequent thermal desorption. Based on these data and high resolution electron energy loss studies[26], benzene is primarily molecularly adsorbed in a similar fashion as that proposed for Ni(111).

Experiments analogous to those described for benzene were performed with toluene. Toluene is irreversibly adsorbed on all five of the nickel surfaces studied at 25°C. No intact toluene could be desorbed thermally or by displacement with trimethylphosphine or methyl isocyanide. The thermal decomposition of perdeutero-toluene yielded D_2 as a decomposition product (Figure 8) with carbon remaining on the nickel surface.

The deuterium (D_2) profile obtained from thermal decomposition of C_7D_8 adsorbed on Ni(111) contained desorption maxima at ≈130°C and ≈185°C. Decomposition of C_7D_8 adsorbed on the stepped Ni 9(111)x(111) and stepped-kinked Ni 7(111)x(310) surfaces yielded results essentially identical to those for Ni(111). The D_2 profile obtained from decomposition of perdeutero-toluene-Ni(100) was qualitatively the same with the D_2 maxima appearing at ≈110°C and ≈240°C. A single desorption peak of D_2 at ≈170°C was produced

Figure 8. The D_2 desorption profiles obtained from thermal decomposition of perdeuterotoluene on the five nickel surfaces studied are shown here. The topmost profile, "c", is that obtained for the Ni(111) surface with the two D_2 desorption maxima occurring at 130°C and 185°C. An essentially identical decomposition spectrum was obtained for the stepped Ni 9(111)x(111) and stepped-kinked Ni 7(111)x(310). Curve "b" was obtained from the thermal decomposition of C_7D_8 on Ni(110) with a single D_2 desorption maximum observed at 150°C. Two D_2 desorption peaks were observed at 110°C and 230°C when perdeuterotoluene was decomposed on a Ni(100) surface as shown in "a". The C_7D_8 exposures in the three cases were (a) 0.2 L., (b) 0.5 L. and (c) 0.5 L. at a crystal temperature of 25°C.

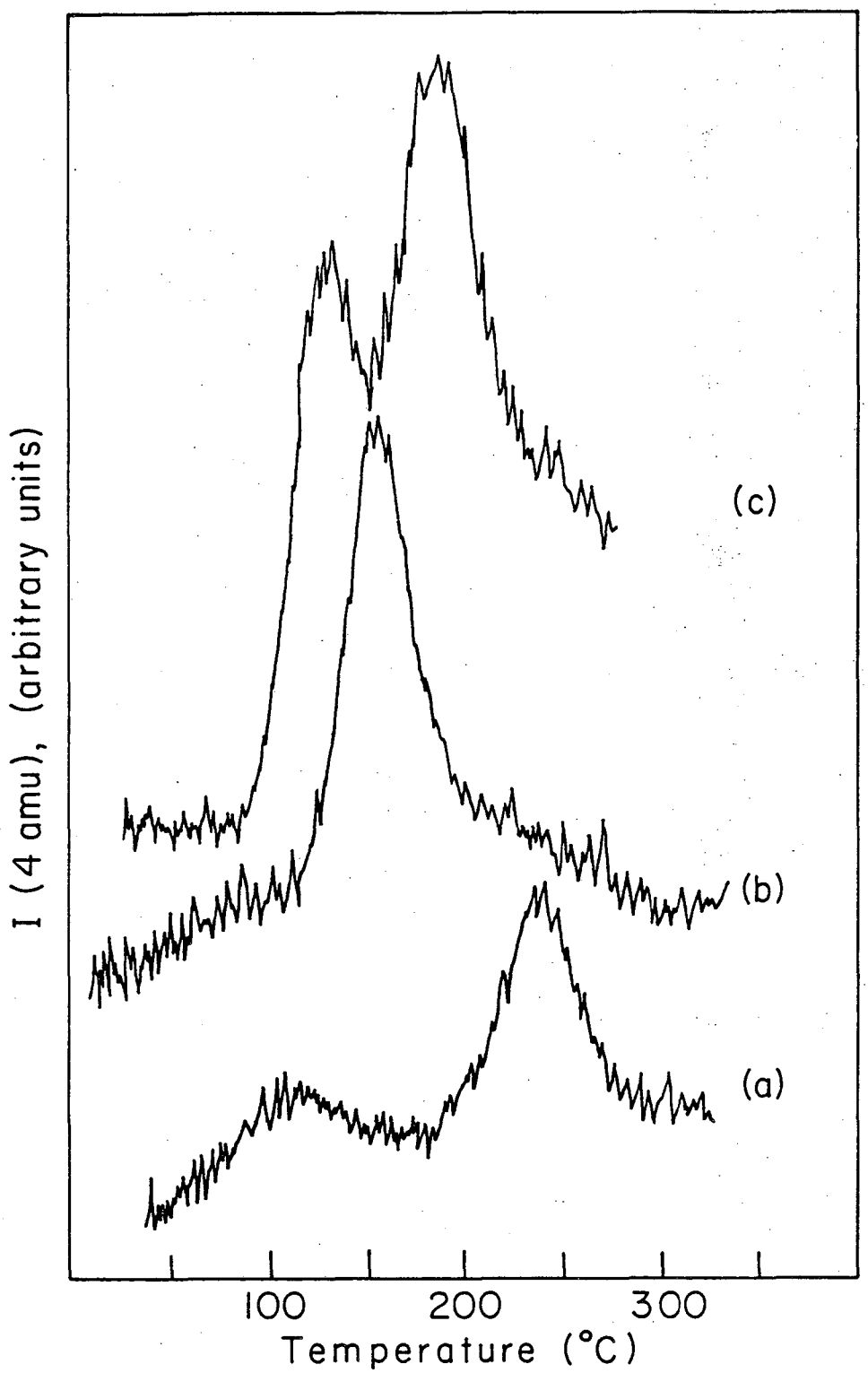

Figure 8.

XBL806-5309

from the decomposition of C_7D_8 on Ni(110).

The qualitative difference in chemisorptive behavior of benzene and toluene is suggestive of a significant interaction of the methyl group with the nickel surfaces. The lower temperature D_2 desorption peak is within the temperature range of that expected for recombination and desorption of free deuterium for all of those surfaces where a double desorption maximum was observed. The partially labelled compounds, $CD_3C_6H_5$ and $CH_3C_6D_5$, were thermally decomposed on all of the surfaces studied. Thermal decomposition of $CD_3C_6H_5$ yielded only the lower temperature D_2 decomposition peak and $CH_3C_6D_5$ only the higher temperature peak on the Ni(111), Ni 9(111)x(111), Ni 7(111)x(310) and Ni(100). (Figures 9, 10.) In addition, the accompanying H_2 decomposition peaks were observed only at high temperature for $CD_3C_6H_5$ and low temperature for $CH_3C_6D_5$ on all four surfaces.[29] No significant differences in the thermal decomposition profiles of C_7D_8, $CD_3C_6H_5$ and $CH_3C_6D_5$ were observed on Ni(110).

In order for such facile C-H bond cleavage to occur, one or more of the methyl hydrogen atoms must interact with the nickel surface upon adsorption on the (111), 9(111)x(111), 7(111)x(310) and (100) surfaces. Two possible models for toluene adsorption on nickel surfaces are shown in Figure 11. In both structures, the aromatic ring is π-coordinated to the nickel surface as for benzene. The methyl hydrogen atoms may coordinate to the surface via a C-H-Ni bridging interaction with toluene remaining molecularly intact. Alternatively, a methyl carbon-hydrogen bond may be cleaved upon adsorption yielding a planar benzyl species and atomic hydrogen adsorbed on the surface. The chemical studies described herein cannot distinguish between these models. The effect of steps and

Figure 9. Selectively labelled toluenes, $CD_3C_6H_5$ and $CH_3C_6D_5$, were thermally decomposed on Ni(111). Single D_2 desorption peaks were obtained at 130°C and 185°C for d_3-and d_5- toluene, respectively, as shown in this figure. Essentially, identical results were obtained for the Ni 9(111)x(111) and Ni 7(111)x(310). Initial adsorption was carried out at approximately 25°C with exposures of 0.3 L. of $CD_3C_6H_5$ and 0.2 L. of $CH_3C_6D_5$.

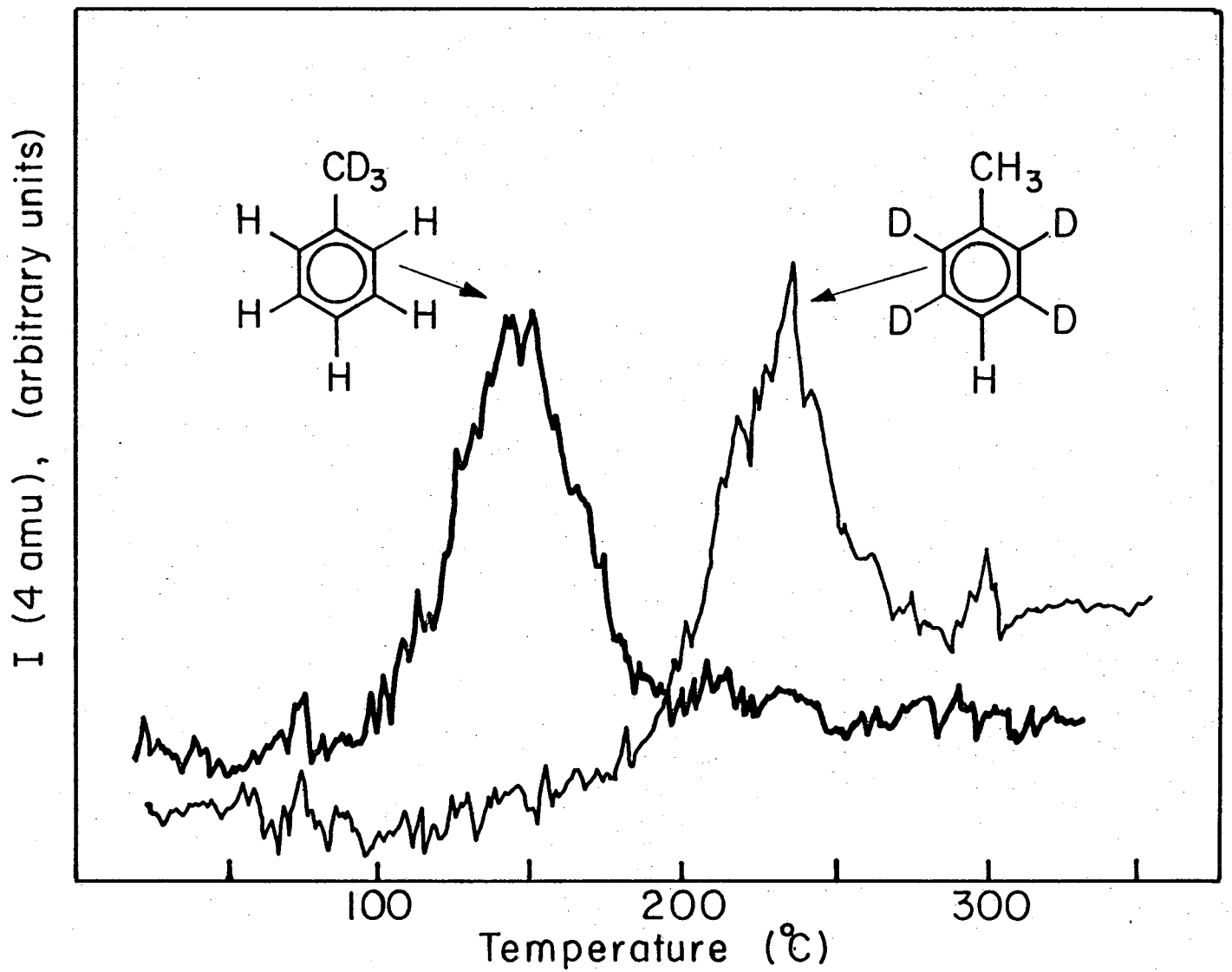

Figure 9.

XBL 804-9446

Figure 10. Qualitatively similar results to the (111) case were obtained when the partially labelled toluenes were thermally decomposed on a Ni(100) surface. The D_2 desorption maxima for decomposition of $CD_3C_6H_5$ and $CH_3C_6D_5$ are observed at 110°C and 230°C as shown in the upper and lower curve, respectively. The approximate exposures in the two cases were 0.2 L. for both $CD_3C_6H_5$ and $CH_3C_6D_5$ at an adsorption temperature of 25°C.

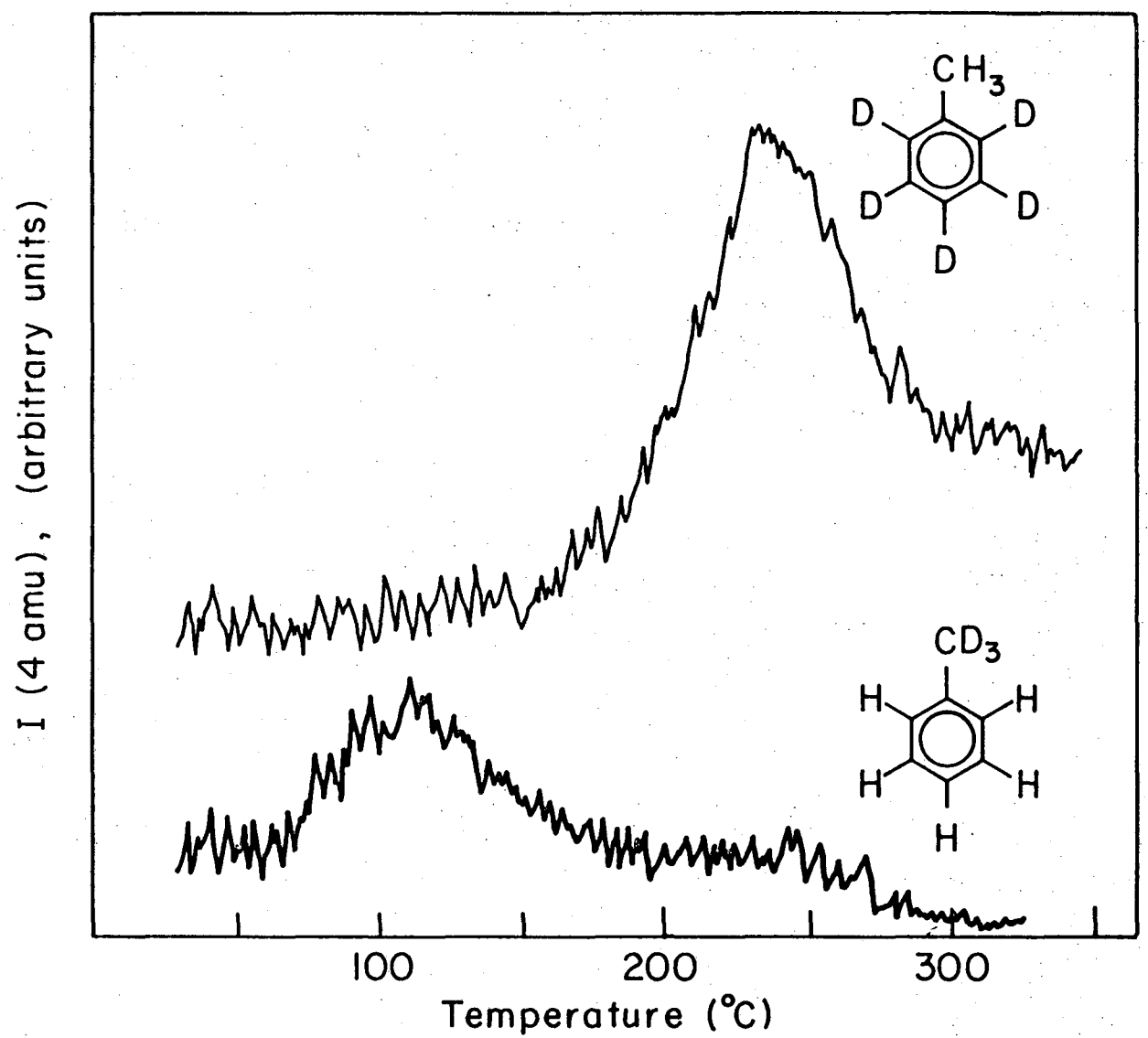

Figure 10.

XBL 806-5308

Figure 11. Two models for toluene adsorption on nickel surfaces that are consistent with the chemistry observed are shown in this figure. On the left, the toluene molecule remains intact with the aromatic ring coordinating in a π-fashion with the C_6 plane essentially parallel to the metal surface. This necessarily brings one or more of the methyl hydrogen atoms in close proximity to the metal surface forming C-H-Ni bridges thus facilitating C-H bond cleavage. Alternatively, as depicted on the right, a methyl hydrogen atom may have been abstracted upon initial chemisorption forming a fully planar benzyl species on the surface.

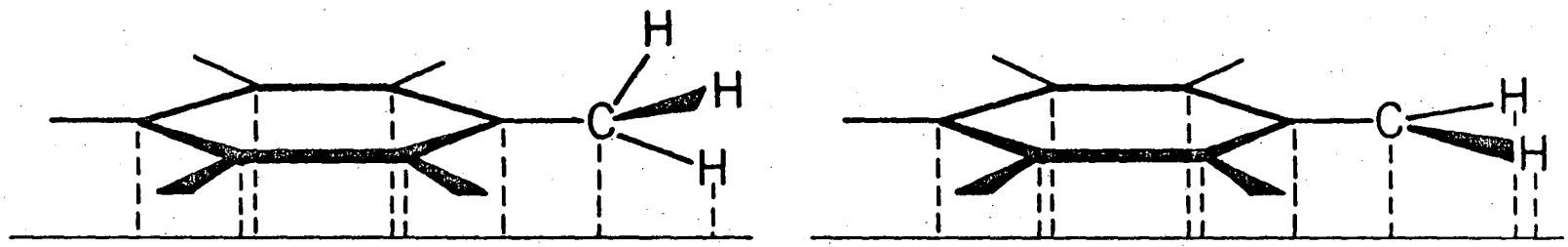

Figure 11.

XBL 817-10648

kinks, as observed for benzene, is not important in the toluene case as the dominant C-H-Ni bridging interaction that activates alkyl C-H bonds occurs readily on flat surfaces.

Carbon, sulfur and oxygen surface impurities all lowered the sticking coefficient of benzene and toluene on nickel at room temperature. The arene sticking probability was negligible on a nickel surface with oxygen contaminant atoms, rendering chemical studies in ultra-high vacuum impossible. The effect of carbon and sulfur was less dramatic; no qualitative change in the benzene or toluene chemisorptive behavior was observed. The surface carbon and sulfur appeared to block chemisorption sites without qualitatively altering the surface chemistry. On the basis of these studies, the same structures for benzene and toluene chemisorption are proposed on the carbon and sulfur contaminated surfaces as for the clean nickel surfaces.

2. Conclusions

In this study, several key factors controlling C-H bond cleavage in aromatic hydrocarbons adsorbed on Ni surfaces have been characterized. These studies suggest that close approach of one or more hydrogen atoms in the molecule to the nickel surface is necessary for C-H bond activation. The effect of surface irregularities on C-H bond activation in benzene is evidence supportive of this view. The qualitative difference in the chemistry of toluene compared to benzene is a more dramatic illustration of this point. Coordination of the aromatic ring of toluene to the nickel surface will necessarily bring one or more methyl hydrogen atoms in close proximity to the surface. The methyl carbon-hydrogen bonds are activated by formation of a C-H-Ni multicenter bridging interaction. This chem-

istry is analogous to that to that observed in organometallic compounds.[30]

Additionally, these studies are suggestive of a novel catalytic approach which can be used as a means of controlling the selectivity of reactions that occur at aromatic versus aliphatic carbon centers. A catalyst with relatively flat surfaces (e.g. sintered films) should be relatively selective towards reaction of the alaphitic function with the rate of reaction being significantly higher for toluene versus benzene. In fact, results supportive of this argument have been obtained for H-D exchange reactions of benzene and toluene.[31] Irregular surfaces (e.g. Raney nickel) should be relatively nonselective, with comparable rates of H-D exchange in benzene and toluene. This has been experimentally born out as reported previously.[12] Thus, in this case, the chemistry observed under ultra-high vacuum conditions is relevant to real catalytic conditions.

V. REACTIVE STUDIES OF C_6-CYCLOHYDROCARBONS ON NICKEL SURFACES

The dehydrogenation of C_6-cyclohydrocarbons to form benzene is known to be catalyzed by nickel metal. The nickel surface chemistry of the reaction product, benzene, is well-characterized as described in the previous chapter allowing for a careful study of the dehydrogenation reaction itself. Surface physics and chemistry used in conjunction with isotopic labelling experiments have delineated some mechanistic details of the dehydrogenation at temperatures above 25°C.

These studies were performed as a function of surface crystallography with the three low-Miller index planes Ni(111), Ni(110) and Ni(100) being utilized. Under these conditions, no significant C-H bond cleavage processes were operative for benzene chemisorbed on these surfaces. Thus, isotopic exchange experiments would identify any reversible C-H bond cleavage processes that may occur in the course of the reaction. The surface composition was also varied with carbon being introduced as a surface impurity, and the dehydrogenation reaction was studied.

1. Results and Discussion

A. Cyclohexane

The surface chemistry of cyclohexane adsorbed on nickel could not be investigated under ultra-high vacuum conditions as its sticking coefficient was essentially zero at 0-200°C for the three low Miller index planes. The range of adsorption temperatures were 0-70°C, 25-200°C and 20-90°C for the Ni(111), Ni(100) and Ni(110), respectively. No higher adsorption temperatures were attempted because benzene itself would irreversibly decompose on the surface under these conditions, as described in the previous chapter. This is consistent with the report by Demuth, et.al.[32] of

a cyclohexane thermal desorption maximum of 170 K (-100°C) on Ni(111). The thermal desorption was reported as being quantitatively reversible, i.e. no reaction occurred on the surface under these conditions. These results are suggestive of a high energy of activation for abstraction of the first aliphatic hydrogen atoms in cyclohexane. "Real world" catalytic studies are typically performed under significantly higher pressures and temperatures in order to increase surface contact times.[33]

B. Cyclohexene

The dehydrogenation of cyclohexene to form benzene was studied on Ni(111), Ni(100) and Ni(110). Cyclohexene had a sticking coefficient comparable to benzene under the same conditions.[34] No detectable benzene was thermally desorbed from the Ni(111) surface following adsorption of c-C_6H_{10}; only an unresolved double hydrogen maximum was observed in the temperature range of 140-200°C. Trimethylphosphine has been shown to completely displace molecular benzene from the Ni(111) surface as described in the previous chapter. As a result, displacement may be used in this case to probe for the reaction product, benzene, without increasing the surface temperature following cyclohexene adsorption. Displacement of a significant amount of C_6D_6 by trimethylphosphine was effected at 65°C following adsorption of C_6D_{10}. The extent of the displacement could not be determined by the amount of deuterium incorporation into the decomposition products of the $P(CH_3)_3$ following displacement subsequent to perdeuterocyclohexene adsorption because adsorbed deuterium atom is a reaction product. Thus, any deuterium present as a result of unreacted or irreversibly adsorbed c-C_6D_{10} would not be detected separately. The dehydrogenation reaction must be

significant since the amounts of benzene detected in the displacement reactions following adsorption of benzene and cyclohexene were comparable.

Based on these results, the dehydrogenation of cyclohexene coordinated to a Ni(111) surface appears to be relatively facile. One possible model for cyclohexene adsorption that is consistent with the observed chemistry is shown in Figure 12. Initial chemisorption most likely occurs via the π-system of the double bond. This will bring one or more hydrogen atoms on adjacent carbon centers in close proximity to the nickel surface. Using the same reasoning as for arene chemisorption, the formation of C-H-Ni bridging interactions would then facilitate C-H bond cleavage.

The thermal desorption profile obtained subsequent to cyclohexene adsorption on Ni(100) contained peaks for cyclohexene, benzene and hydrogen at 100°C, 220°C and 93, 216°C (double maximum), respectively. Benzene itself thermally desorbs near 220°C on this surface and is accompanied by the least amount of decomposition. The desorption of cyclohexene itself may be a result of a lower rate of dehydrogenation of this surface compared to Ni(111). The H_2 desorption maximum observed at 93°C is in the range for that expected for adsorbed hydrogen on the Ni(100) surface.[33] Thermal desorption of a 1:1 mixture of c-C_6H_{10} and c-C_6D_{10} yielded only C_6H_{10}, C_6D_{10}, C_6H_6, and C_6D_6. No isotopic mixing was observed indicating that no significant reversible C-H bond breaking processes were operative in the mechanism for benzene formation from cyclohexene.[34] On the basis of these results, it is clear that a significant fraction of the cyclohexene adsorbed on both the Ni(111) and Ni(100) surfaces dehydrogenates to form benzene at relatively low temperatures.

Figure 12. One possible model for cyclohexene coordinated to a flat nickel surface is illustrated here. Initial chemisorption presumably occurs through the π-system allowing for C-H-Ni bridge bond formation with the hydrogen atoms on adjacent carbon atoms. These C-H bonds would, therefore, be activated allowing for facile dehydrogenation. The chair conformation is depicted here, but a similar model may be drawn for the boat conformation without affecting the possibility of C-H-Ni interactions.

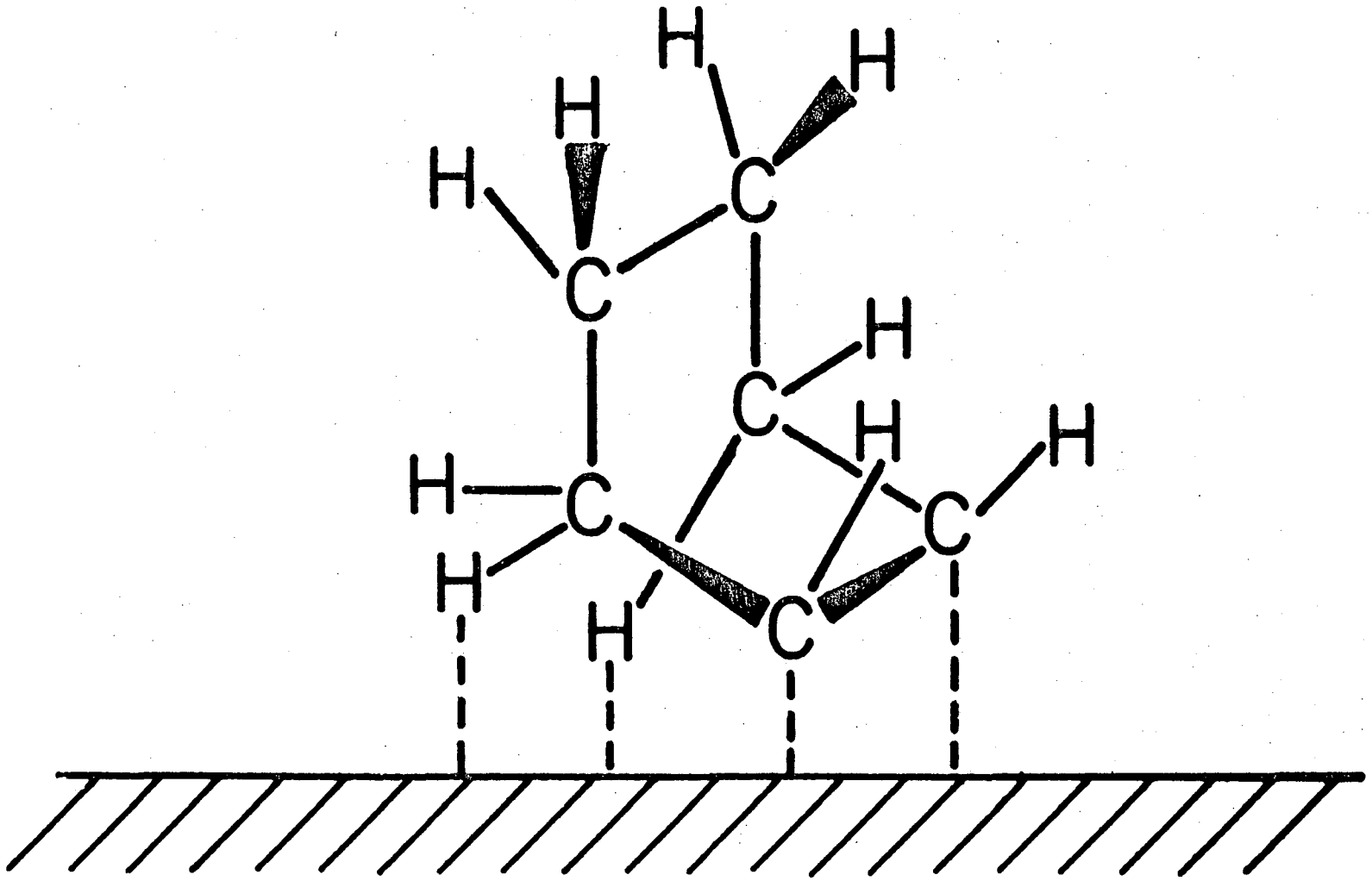

Figure 12.

XBL 815-9480

Cyclohexene adsorbed on Ni(110) exhibits markedly different chemistry than on the Ni(111) and Ni(100) surfaces. Thermal desorption following adsorption of c-C_6H_{10} on clean Ni(110) yielded a double hydrogen maximum at 100°C and 200°C in addition to a trace of C_6H_6 at 200°C. The temperature where the maximum rate of desorption is obtained for benzene itself is 100°C as reported in the previous chapter of this thesis. Chemical displacement of a small amount of benzene by $P(CH_3)_3$ was observed following adsorption of cyclohexene at 25°C. Subsequent thermal desorption still yielded some benzene. The displacement results clearly show that some benzene is formed upon initial adsorption. The thermal desorption experiments demonstrate that a significant fraction of the adsorbed cyclohexene reacts to form benzene via a pathway with an activation barrier higher than the energy of desorption. Thermal reaction of a mixture of c-C_6H_{10} and c-C_6D_{10} yielded only C_6H_6 and C_6D_6 as products. Thus, reversible C-H bond cleavage can be mechanistically ruled out for this reaction. The higher activation energy for benzene formation on the Ni(110) surface as compared to the Ni(111) and Ni(100) surfaces cannot be readily accounted for on the basis of these experiments.

The presence of surface carbide on Ni(110) significantly lowered the activation barrier for the major benzene formation pathway from cyclohexene. The amount of benzene thermally desorbed from the carbided surface was larger by approximately a factor of two compared to the clean Ni(110) surface and the desorption temperature was decreased to 134°C. The displacement behavior was essentially the same as that for clean Ni(110) and no cross-labelled products were obtained from reaction of a C_6H_{10} and C_6D_{10} mixture. The change

in cyclohexene chemistry on the Ni(110) surface is in sharp contrast to the Ni(111) and Ni(100) cases where no significant difference between clean and carbided surfaces were observed. The role of the surface carbide is not understood, but direct rehydrogenation to form benzene can be ruled out on the basis of the mixed isotope experiments. Therefore, the carbide is probably changing the electronic character of the Ni(110) surface.

C. 1,3- and 1,4-Cyclohexadiene

The chemistry of 1,3- and 1,4-cyclohexadiene was similar to that observed for cyclohexene on all three surfaces studied. The only qualitative difference observed was on Ni(111) where some benzene could be thermally desorbed following adsorption of 1,3- and 1,4-cyclohexadiene in the temperature range of 25-75°C. These results are suggestive of similar reaction pathways for the dehydrogenation of cyclohexene and the cyclohexadienes. The cyclohexadienes readily react to form benzene on Ni(111) and Ni(100). Adsorbed cyclohexadiene may be a reaction intermediate in the Ni(110) case where complete reaction to form benzene does not occur until 200°C. These results are suggestive of simple stepwise C-H bond scission to form adsorbed benzene on nickel surfaces. The limiting step in the overall reaction, C_6H_{12} to form C_6H_6, appears to be initial hydrogen atom abstraction from cyclohexane. Presumably, initial chemisorption occurs via the π-system bringing one or more hydrogen atoms in close proximity to the nickel surface, analogous to the proposed model for cyclohexene adsorption. Coordinated cyclohexediene may be a model for a surface intermediate in the dehydrogenation process.

2. Conclusions

The dehydrogenation reactions of several C_6-cyclohydrocarbons to form benzene have been studied on the low Miller index surfaces of nickel above temperatures of 25°C using ultrahigh vacuum techniques. The fully saturated molecule, cyclohexane, did not significantly interact with these surfaces under the conditions of these studies. In contrast, c-C_6H_{10} and 1,3- and 1,4-c-C_6H_8 readily dehydrogenated to form a significant amount of benzene at room temperature. This suggests a mechanism in which initial coordination and initial C-H bond scission of the cyclohexane is the step with the highest activation barrier. The facile dehydrogenation of c-C_6H_{10} and c-C_6H_8 and the absence of reversible C-H bond cleavage suggests a model in which there is simple stepwise hydrogen atom abstraction to form benzene following coordination via the double bond of these molecules. Carbon-hydorgen bond activation is proposed to occur via formation of a multicenter C-H-Ni bridging interaction.

VI. NICKEL SURFACE COORDINATION CHEMISTRY OF METHYL ISOCYANIDE AND ACETONITRILE

The adsorption of the isomeric molecules, CH_3CN and CH_3NC, on Ni(111) has been studied previously.[11] In this work, the nickel surface chemistry of these molecules have been investigated as a function of surface crystallography and composition. Five different crystallographic planes, the three low Miller index surfaces (Figure 1), the stepped Ni 9(111)x(111) and the stepped-kinked Ni 7(111)x(310) (Figures 2 and 3, respectively) have been utilized with carbon, sulfur and oxygen introduced as surface impurities.

The presence of carbon on the nickel surfaces qualitatively altered the chemistry of CH_3NC such that it was similar to that observed for its isomer, CH_3CN. This was suggestive of a surface catalyzed isomerization of CH_3NC to form the thermodynamically stable isomer, CH_3CN. The catalytic isomerization was, in fact, observed over Raney nickel and evaporated nickel film catalysts.

High resolution electron energy loss studies were performed for both acetonitrile and methyl isocyanide adsorbed on Ni(111) and Ni(111)-C. The vibrational data helped to delineate the adsorption structures of the isomers and the effect of the surface carbide.

1. Results and Discussion

A. Acetonitrile: Room Temperature Adsorption

Acetonitrile adsorbed at 25°C was largely thermally reversible on all of the nickel surfaces studied with the exception of Ni(110). The presence of submonolayer amounts of sulfur or carbon atoms did not qualitatively alter the desorption characteristics of the nitrile although the sticking coefficient was significantly lowered.[35] Surface contaminant oxygen atoms so greatly reduced the acetonitrile

sticking coefficient that this chemistry could not be explored under ultra high vacuum conditions.

Acetonitrile formed an ordered p(2x2) structure when chemisorbed on Ni(111) near 25°C. The thermal desorption was nearly quantitative with small amounts of the decomposition products, H_2 and N_2, being desorbed at 150°C and 550°C, respectively. Trace amounts of carbon and nitrogen remained on the surface following the thermal desorption experiments. Quantitative displacement[36] of the nitrile could be effected at 25°C by using $P(CH_3)_3$ or CO. Thermal desorption following coadsorption of a 40:60 mixture of $CH_3C^{15}N$ and CD_3CN yielded no isotopically mixed products. Similarly, no isotopically mixed products were obtained when a mixture of $CH_3C^{15}N$ and CD_3CN were displaced using CO or $P(CH_3)_3$. Thus, acetonitrile must be a single, molecularly (non-dissociatively) bound state on the Ni(111) surface up to the thermal desorption temperature of 90°C. Acetonitrile chemistry on the stepped Ni 9(111)x(111) and stepped-kinked Ni 7(111)x(310) were studied in an analogous fashion. The acetonitrile surface chemistry was essentially the same as on the Ni(111) surface. The only difference was a larger degree of thermal decomposition on the stepped and stepped-kinked surfaces. The estimated amount of decomposition was 1-2% for Ni(111), 5% for Ni 9(111)x(111) and 15% for the Ni 7(111)x(310).

Acetonitrile chemisorption was the least reversible in a thermal context on the super-stepped Ni(110) surface. The thermal desorption maximum for the nitrile was observed at 110°C with the accompanying H_2 decomposition peak occuring in the range 110-120°C. No isotopic mixing was observed in a thermal desorption experiment using a mixture of CD_3CN and $CH_3C^{15}N$. The presence of surface carbon did

not alter the acetonitrile surface chemistry. No desorption of the nitrile could be effected using $P(CH_3)_3$ or CO as displacement gases at 25°C.

Acetonitrile chemisorption on the flat Ni(100) surface was partially thermally reversible with ~15% of the nitrile decomposing during a thermal desorption experiment. An ordered c(2x2) structure was formed on the Ni(100) surface following adsorption of CH_3CN at 25°C. Isotopic labelling studies demonstrated that neither reversible or irreversible bond breaking was a significant process for the fraction of the acetonitrile that thermally desorbed. Trimethylphosphine displaced the nitrile at room temperature but CO was ineffective as a displacing agent. Surface carbide did not qualitatively alter this chemistry.

On the basis of the chemical information obtained, some structural and mechanistic characteristics of acetonitrile adsorbed on nickel surfaces may be proposed. All the physical and chemical data are suggestive of acetonitrile bound on Ni(111) via the nitrogen atom with the CN vector essentially perpendicular to the metal surface. (See Figure 13.) This type of structure does not readily allow for a significant degree of C-H-Ni interaction accounting for the thermally reversible character of CH_3CN adsorption. The diffraction data also supports this hypothesis. If the CN vector were canted with respect to the surface, orientational disorder would be expected, giving rise to a larger unit cell. Additionally, the van der Waal's radii of adjacent methyl groups would overlap for a tilted structure. In the Ni(100) case special constraints dictate bonding via the nitrogen with the CN vector perpendicular to the surface for the c(2x2) structure. Analogous bonding is

found for many mononuclear and polynuclear metal acetonitrile complexes.[38]

The stepped Ni 9(111)x(111) and stepped-kinked Ni 7(111)x(310) surfaces were qualitatively analogous to the flat Ni(111) surface. The only difference was in the variation in the extent of thermal reversibility as a function of crystallography. The degree of thermal decomposition of CH_3CN increased in the order Ni(111)< Ni 9(111)x(111)<Ni 7(111)x(310). Closer approach of the methyl hydrogen atoms of the chemisorbed acetonitrile is possible for step or kink sites as illustrated in Figure 13. Thus, the degree of C-H bond cleavage would be expectedly higher when steps or kinks are present.

The chemistry of acetonitrile adsorbed on the Ni(110) surface at 25°C qualitatively differed from the close packed surfaces. A much larger fraction of the CH_3CN molecules irreversibly decomposed in a thermal desorption experiment. Thus, closer approach of one or more methyl hydrogen atoms to the Ni(110) surface must be postulated. The inability of CO or $P(CH_3)_3$ to displace the CH_3CN from the Ni(110) surface is a further qualitative difference. No detailed structural or stereochemical features can be readily proposed on the basis of this information.

The chemisorptive behavior of acetonitrile adsorbed on the flat, less densely packed Ni(100) surface was distinguished by two features. The thermal desorption temperature maximum was slightly (20°C) higher than that observed from the Ni(111) case and the extent of irreversible decomposition was comparable to the kinked 7(111)x(310) surface. Geometric factors may be responsible for the greater thermal reactivity. The displacement reactions eliminate the

Figure 13. Depicted in this figure are proposed bonding for acetonitrile on nickel surfaces. On the left, the CH_3CN is coordinated to flat terrace atoms with the CN bond vector essentially perpendicular to the terrace plane. In this configuration the C-C-H bond angle must be very acute in order for any C-H-Ni bridge formation. Thus, the degree of C-H bond scission should be small for acetonitrile coordination to flat surfaces. This is the same model proposed for CH_3CN coordinated to the flat low-Miller index nickel surfaces. The two models on the right illustrate how C-H-Ni bridging interactions may be formed on or near step or kink sites. These would allow for a larger extent of decomposition (dehydrogenation) for stepped or stepped-kinked surfaces.

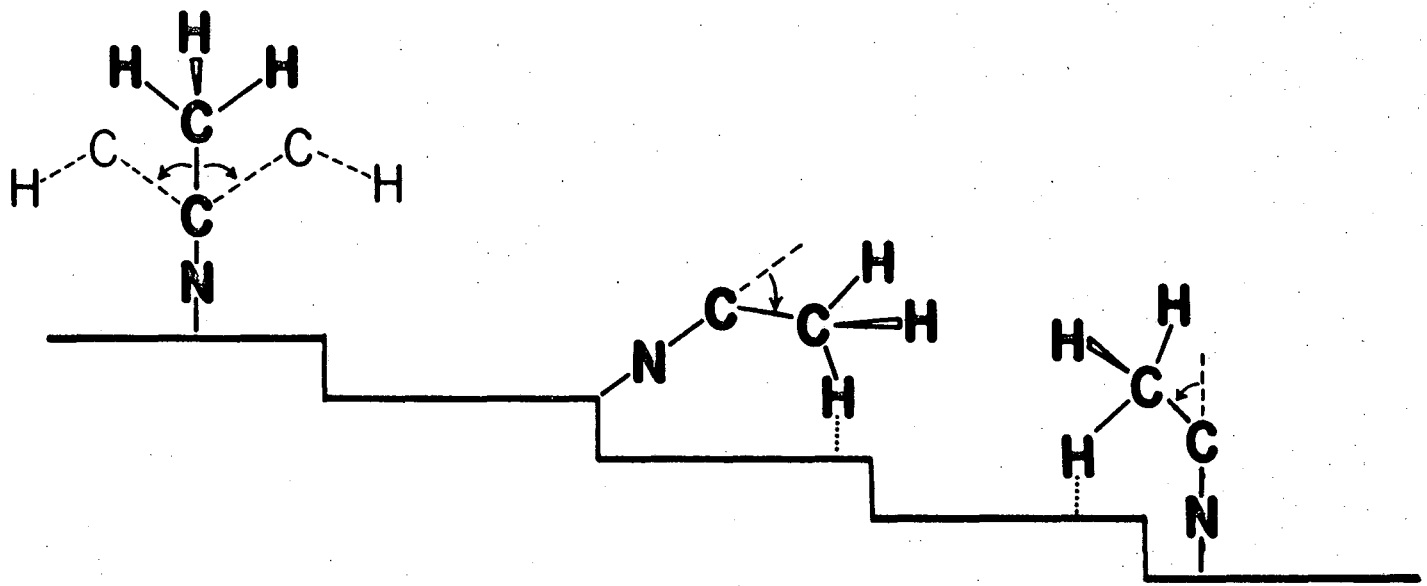

Figure 13.

XBL 804-9447

possibility of dissociative adsorption under these conditions.

B. Methyl Isocyanide: Room Temperature Adsorption

Methyl isocyanide interacted much more strongly with the nickel surfaces than its isomer, acetonitrile. Thus, the nickel surface chemistry associated with CH_3NC was qualitatively different than CH_3CN. The initial sticking coefficient was near unity at room temperature and the isocyanide was irreversibly adsorbed on all nickel surfaces studied. Attempted thermal desorption following adsorption of CH_3NC on the nickel surfaces yielded only a trace amount of mass 41; the major products were H_2, HCN and at temperatures above 500°C, N_2. Surface impurities of S ($\theta \lesssim .3$) did not qualitatively alter this chemistry; only the sticking coefficient was reduced.

The presence of surface carbide qualitatively altered the chemistry observed following adsorption of the isocyanide on all of the nickel surfaces studied. The thermal desorption spectra obtained following adsorption of CH_3NC on carbided nickel surfaces were essentially the same as those obtained for CH_3CN adsorbed on these surfaces as shown in Figures 14-17. The mass 41 thermal desorption maxima for the Ni(111)-C surface were 90°C for both CH_3NC and CH_3CN adsorption. The coincidence of the desorption maxima is suggestive of catalytic isomerization of CH_3NC to form CH_3CN, the thermodynamically stable isomer. A definitive characterization cannot be made based on the mass spectrometric results. Complimentary catalytic studies that supported this postulate were performed and are described in detail later in this section.

Isotopic exchange experiments established that the isomerization was a fully intramolecular process. Thermal desorption of a mixture of $CH_3N^{13}C$ and CD_3NC did not lead to the formation of any cross

labelled products.[39] Furthermore, no ^{13}C incorporation into the product, CH_3CN, was observed when the isocyanide was adsorbed on a Ni(111)-^{13}C surface. Essentially, the same chemistry was associated with methyl isocyanide adsorbed on the stepped Ni 9(111)x(111) surface (Figure 14). The temperature at which isomerization occurred could not be determined. Displacement reactions using CO or $P(CH_3)_3$ were attempted in the temperature range of 25-70°C, following methyl isocyanide adsorption on the carbided surface. No displacement was observed under these conditions. Thus, the isomerization must occur very near 90°C. Clearly, no isomerization occurred up to 70°C or mass 41 (acetonitrile) displacement would have been observed.

The chemistry of methyl isocyanide on the kinked Ni 7(111)x(310) surface was analogous to the (111) case. An additional feature appeared at 150°C in the mass 41 thermal desorption profile for the Ni 7(111)x(310)-C surface as shown in Figure 15. This desorption may either be attributed to unisomerized methyl isocyanide or to acetonitrile that is formed via a pathway with a higher activation barrier. The mass 41 desorption profile obtained from CH_3CN adsorbed on this surface contained only the 90°C maximum. (Figure 15.)

The thermal desorption behavior of CH_3NC adsorbed on Ni(110) and Ni(100) also exhibited a qualitative change upon surface contamination with carbide or carbon and nitrogen. A weak, broad mass 41 desorption was observed from thermal desorption following CH_3NC adsorption on a Ni(110)-C surface. This desorption profile was similar in character to that obtained following acetonitrile adsorption on the carbided Ni(110) surface. (Figure 16.) Isotopic labelling studies using a mixture of CD_3NC and $CH_3N^{13}C$ produced no cross-labelled species in the thermal desporption reaction on Ni(110)-C.

Figure 14. The thermal desorption spectra obtained following adsorption of the isomers, CH_3NC and CH_3CN, on a Ni(111)-C-N surface at 25°C are shown in the figure. The exposures were 0.5 L. and 2.0 L. with approximate carbon coverages[40] of 0.4 and 0.5 of a monolayer prior to exposure for CH_3NC and CH_3CN, respectively.

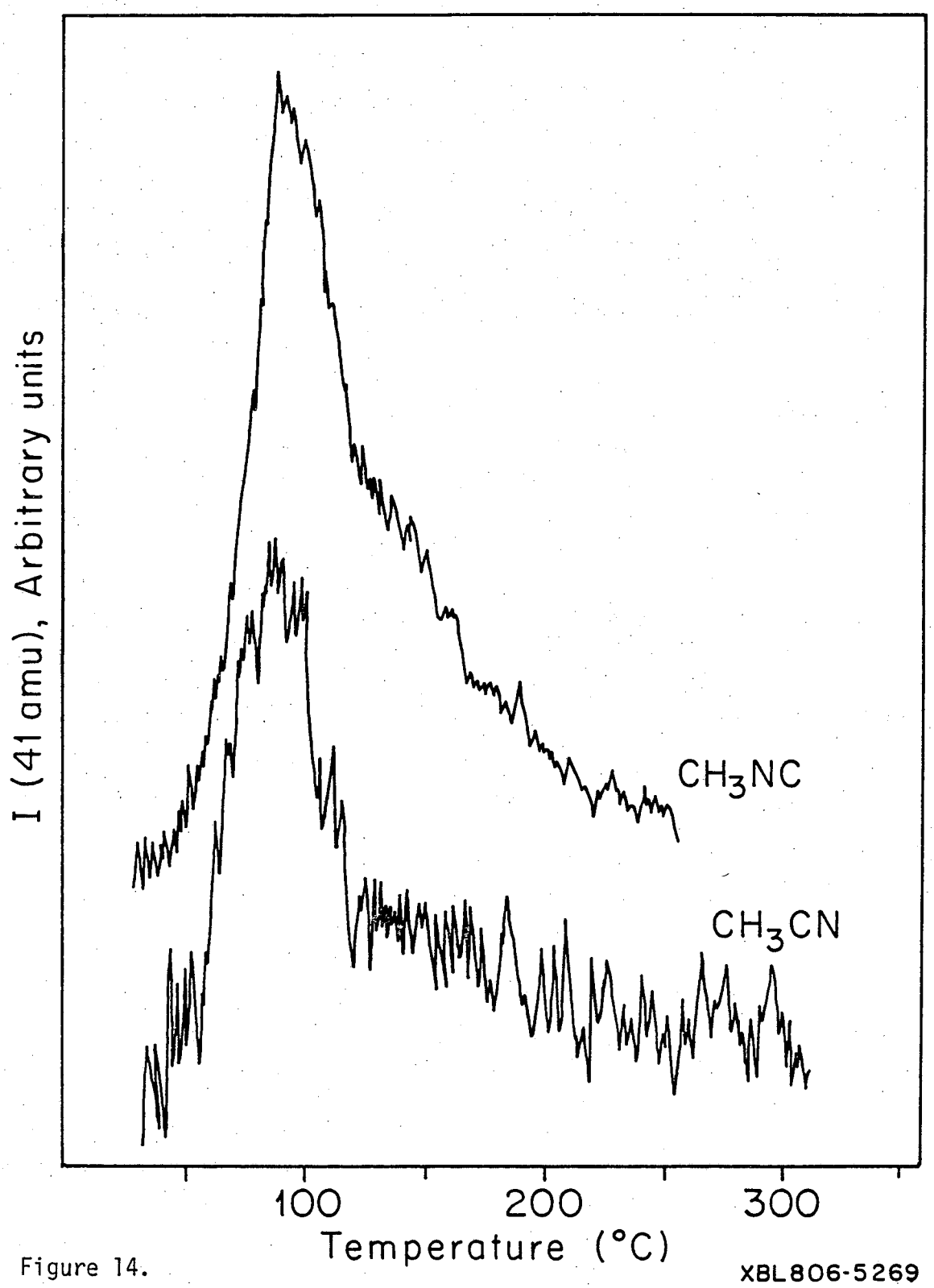
I (41 amu), Arbitrary units
CH3NC
CH3CN
100
200
300
Temperature (°C)
XBL806-5269

Figure 14.

Figure 15. Presented as a parallel to the desorption characteristics of the Ni(111)-C-N surface are the thermal desorption profiles obtained following exposure of a stepped-kinked Ni 7(111)x (310) surface with carbon and nitrogen impurities to 0.2 L. of CH_3NC and 0.2 L. of CH_3CN at 25°C. Approximate carbon coverages[40] prior to adsorption were 0.2 and 0.4 of a monolayer for CH_3NC and CH_3CN, respectively.

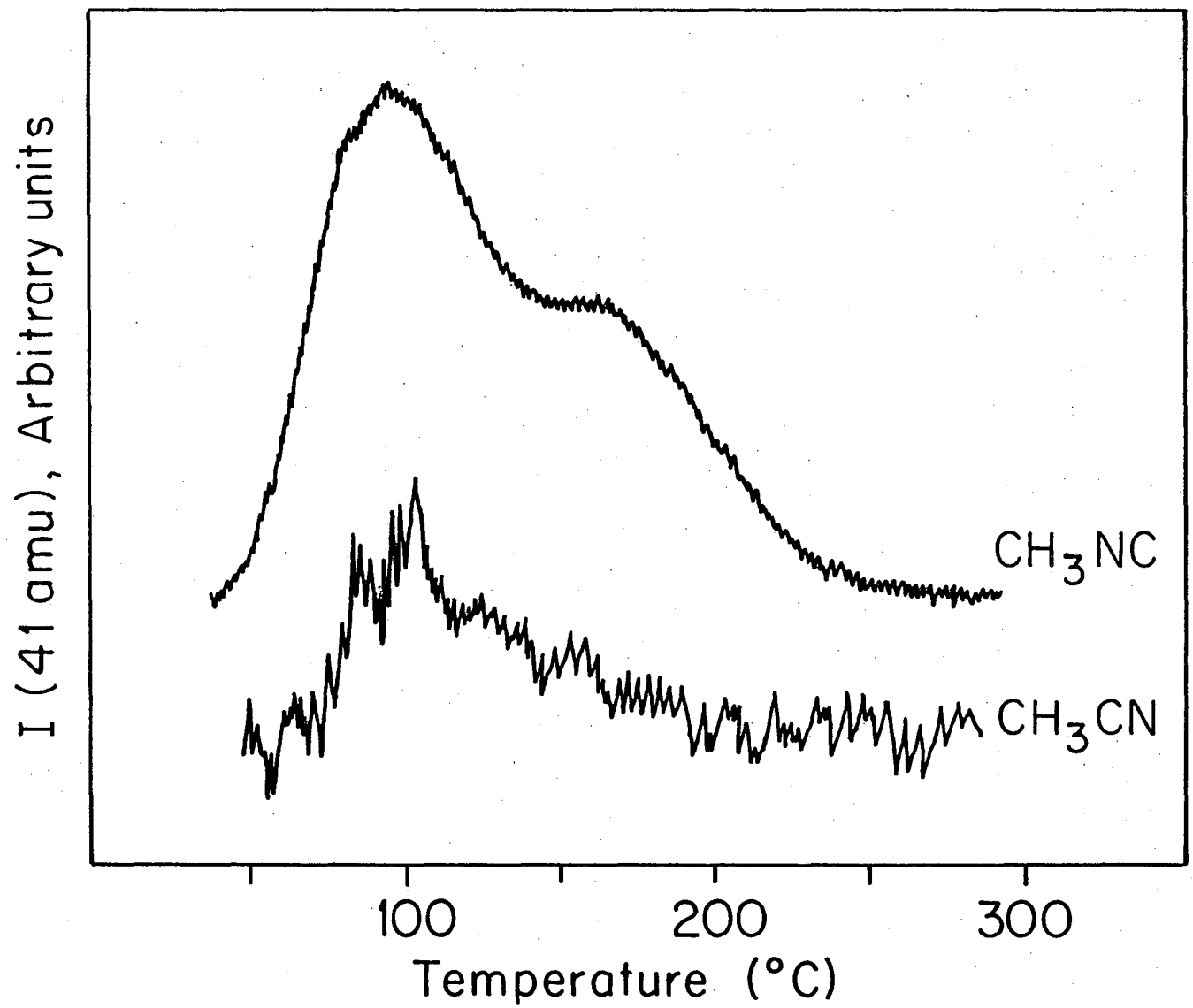

Figure 15.

XBL 806-5267

Figure 16. The mass 41 thermal desorption profiles obtained subsequent to adsorption of 0.2 L. of CH_3NC and 0.8 L. of CH_3CN on a Ni(100)-C-N surface at 25°C are illustrated here for comparison. The approximate carbon coverages[40] prior to exposure were 0.6 and 0.3 of a monolayer for CH_3NC and CH_3CN, respectively.

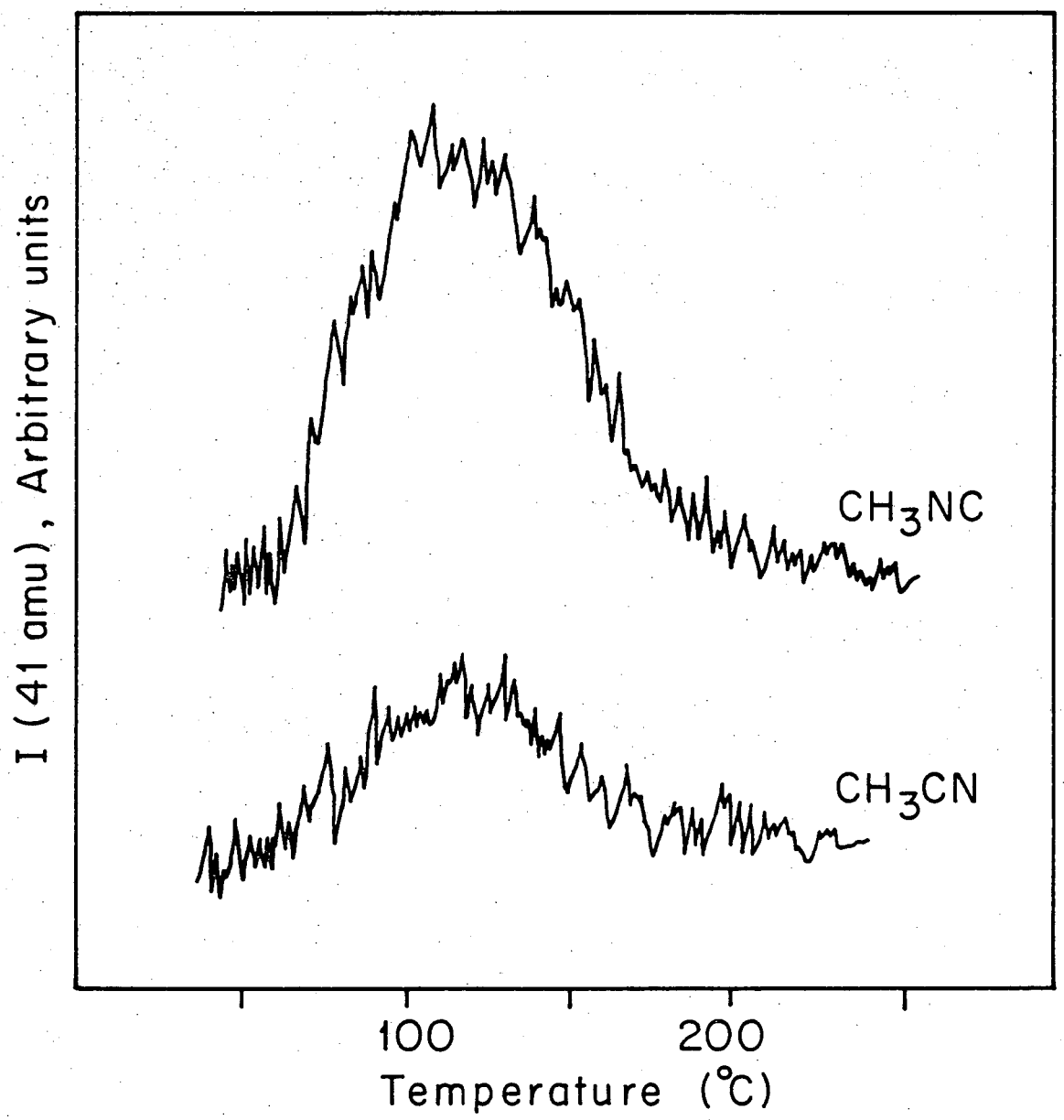

Figure 16.

XBL 806-5268

Figure 17. Comparison of the thermal desorption spectra obtained following adsorption of CH_3NC and CH_3CN at 25°C is made in this figure for a Ni(110)-C-N surface. Estimated carbon coverages[40] were 0.8 and 0.6 of a monolayer for CH_3NC and CH_3CN, respectively.

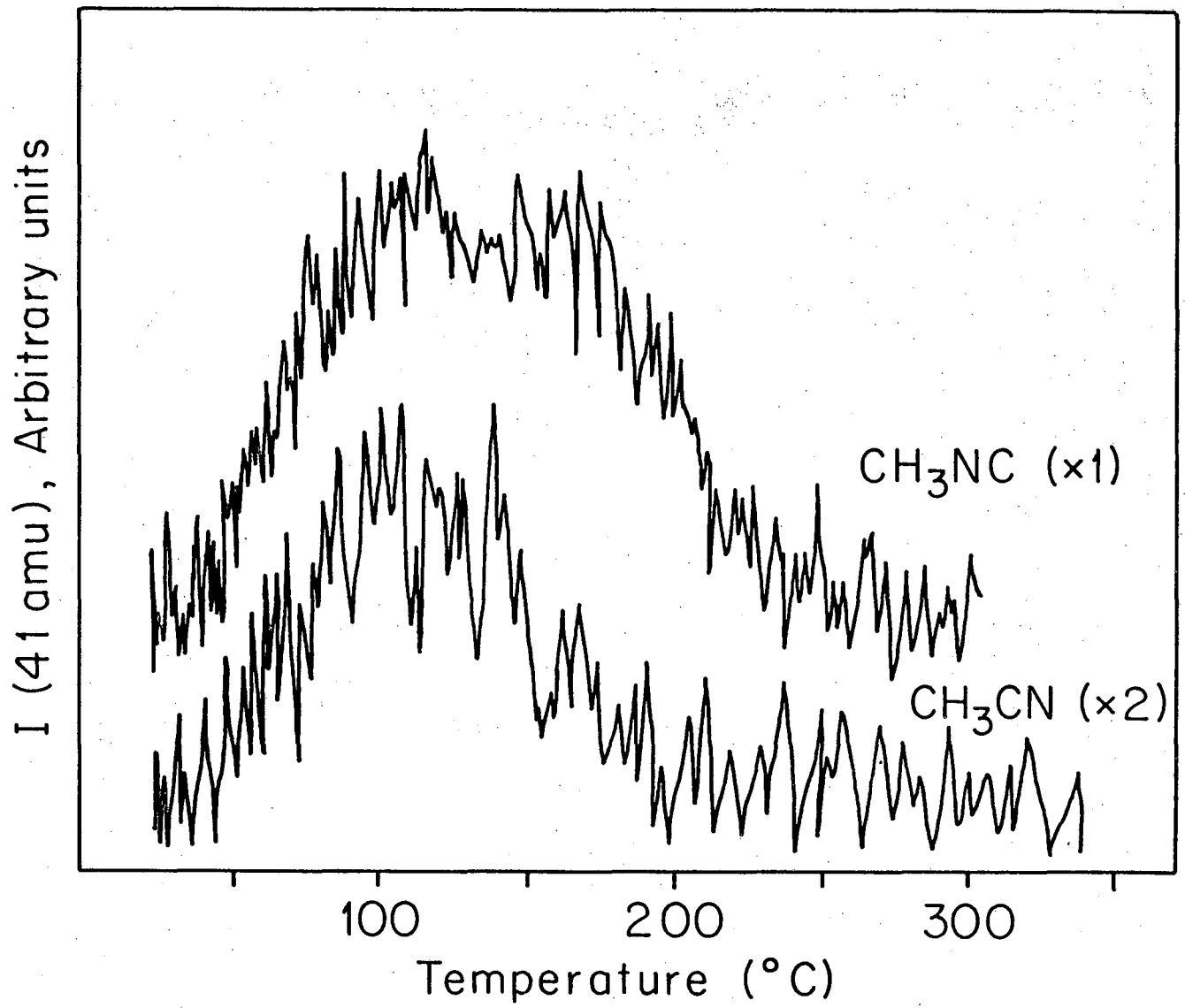

Figure 17.

XBL806-5266

Thermal desorption experiments subsequent to CH_3NC adsorption on a carbided Ni(100) surface produced molecules of mass 41 in the temperature range of 100-160°C (See Figure 17). Mixed isotope studies produced no cross-labelled products. The similarity in the thermal desorption profiles obtained for adsorbed CH_3NC and CH_3CN on the Ni(100)-C surface is suggestive of isomerization.

None of these studies described yields direct structural or stereochemical information about the adsorbed isocyanide. The fact that the CH_3NC chemisorption was irreversible on clean nickel surfaces suggests a significant degree of C-H-Ni bridging interaction. If the N-C bond vector were oriented essentially parallel to the nickel surface plane, one or more methyl hydrogen atoms would be brought in close proximity to the nickel surface, allowing for a significant amount of Ni-H overlap. This type of bridge bonding of the NC group has been established for isocyanide ligands in organometallic clusters.[41]

The role of surface carbon in favoring isomerization versus decomposition is not clearly defined. It most likely perturbs the surface electronic denisty. Clearly, the isomerization is fully intramolecular as in the gas phase case.

C. Catalyst Studies

The thermal isomerization of gaseous CH_3NC is a well-characterized intramolecular reaction. No reports of a catalytic reaction involving metal surfaces were found in the literature. Thus, catalytic studies on a variety of nickel surfaces were studied in order to compliment the ultra-high vacuum studies.

Exposure of liquid CH_3NC to nickel surfaces at temperatures in the range of 50-150°C led to no detectable isomerization after

several hours of reaction time. Raney nickel, bulk granular nickel obtained from reduction of nickel oxide formed from pyrolysis of hydrated nickel nitrate and nickel powder obtained from hydrogenation of bis (1,5-cyclooctadiene) nickel all yielded the same result under these conditions. In some cases, discoloration of the metal surface was observed, suggestive of a polymerization reaction that may deactivate the catalyst. This effect was minimized by performing the catalytic reaction at low CH_3NC pressures (1 torr) with contact times on the order of 5 sec. under flow conditions. The isomerization readily occurred over Raney nickel in the temperature range of 150-200°C.[42] Catalytic isomerization of CH_3NC to CH_3CN was a fast reaction and dominated under these conditions. These experiments demonstrate that carbided nickel surfaces[43] catalyze this isomerization as was postulated on the basis of the ultra-high vacuum studies.

D. Acetonitrile; Vibrational Studies on Ni(111) at - 170°C

The thermal desorption spectrum for acetonitrile adsorbed on Ni(111) and Ni(111)-C at -170°C was significantly different than that described in the previous section for adsorption at 25°C. Several new desorption features were observed when CH_3CN was adsorbed on Ni(111) at -170°C. Three distinct mass 41 desorption peaks could be resolved in the thermal desorption spectrum of a multi-layer of CH_3CN. (Figure 18.) The lowest temperature desorption maximum occurred at -130°C, attributed to sublimation of solid CH_3CN. Two additional desorption peaks occurred at 0°C and 85°C. The relative magnitudes of the 0°C and 85°C desorption peaks varied as a function of coverage with the 85°C peak growing in more rapidly at higher CH_3CN coverages as shown in Figure 19. Both peaks were present in the thermal desorption spectrum obtained following adsorption of

Figure 18. The thermal desorption spectrum obtained following adsorption of a multilayer of CH_3CN on Ni(111) is depicted here. The mass 41 profile corresponds to desorption of molecular acetonitrile with mass 2 and mass 27 profiles for the decomposition products H_2 and HCN, respectively. The heating rate was approximately 10°C/sec.

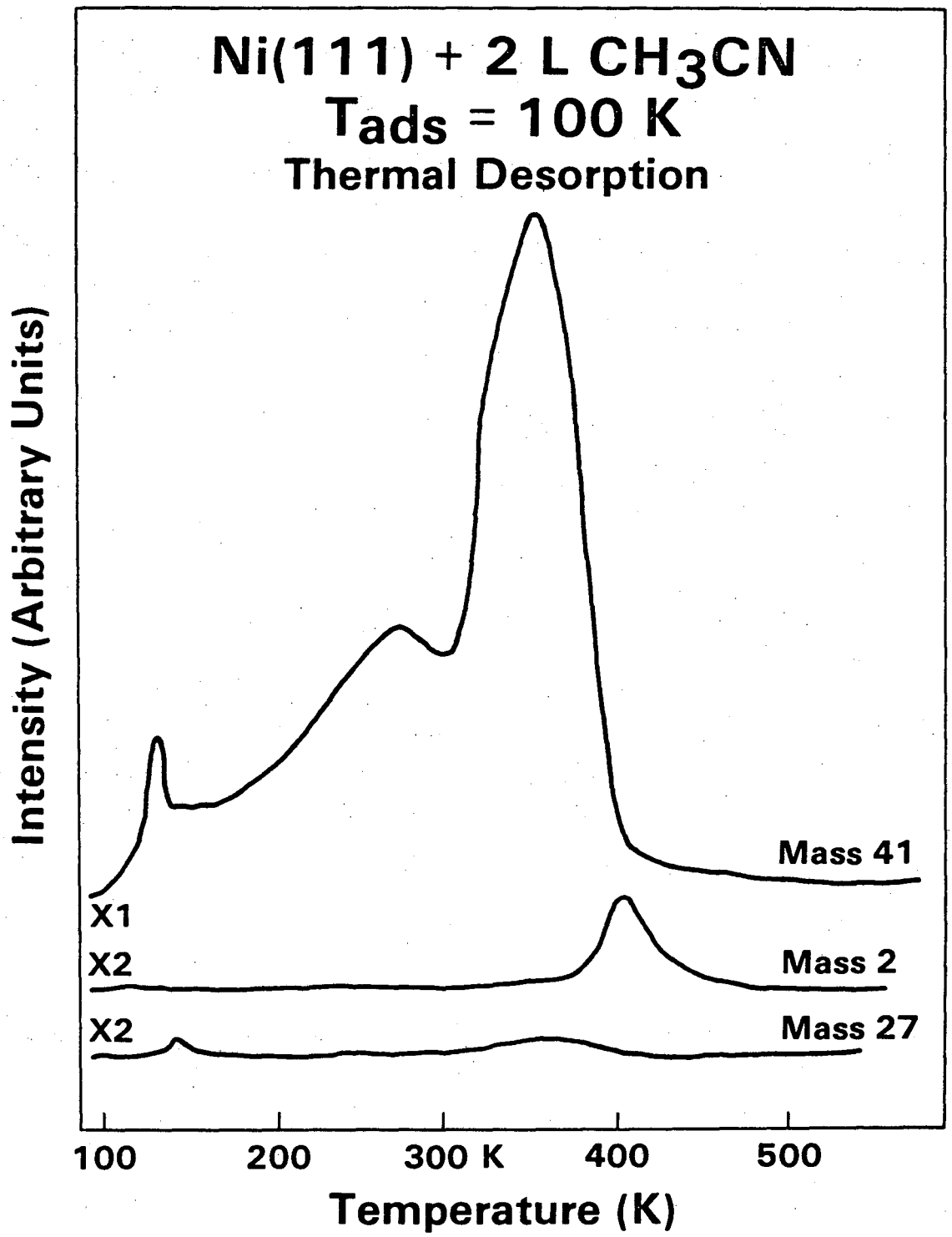

Figure 18.

XBL 817-10658

Figure 19. High resolution electron energy loss spectra obtained as a function of coverage for acetonitrile adsorbed on Ni(111) at -170°C are presented on the left of the figure. The incident beam energy was 2 eV and the resolution (full width at half maximum of the elastic peak) was 10 meV in all cases. The corresponding mass 41 thermal desorption profiles are depicted on the right.

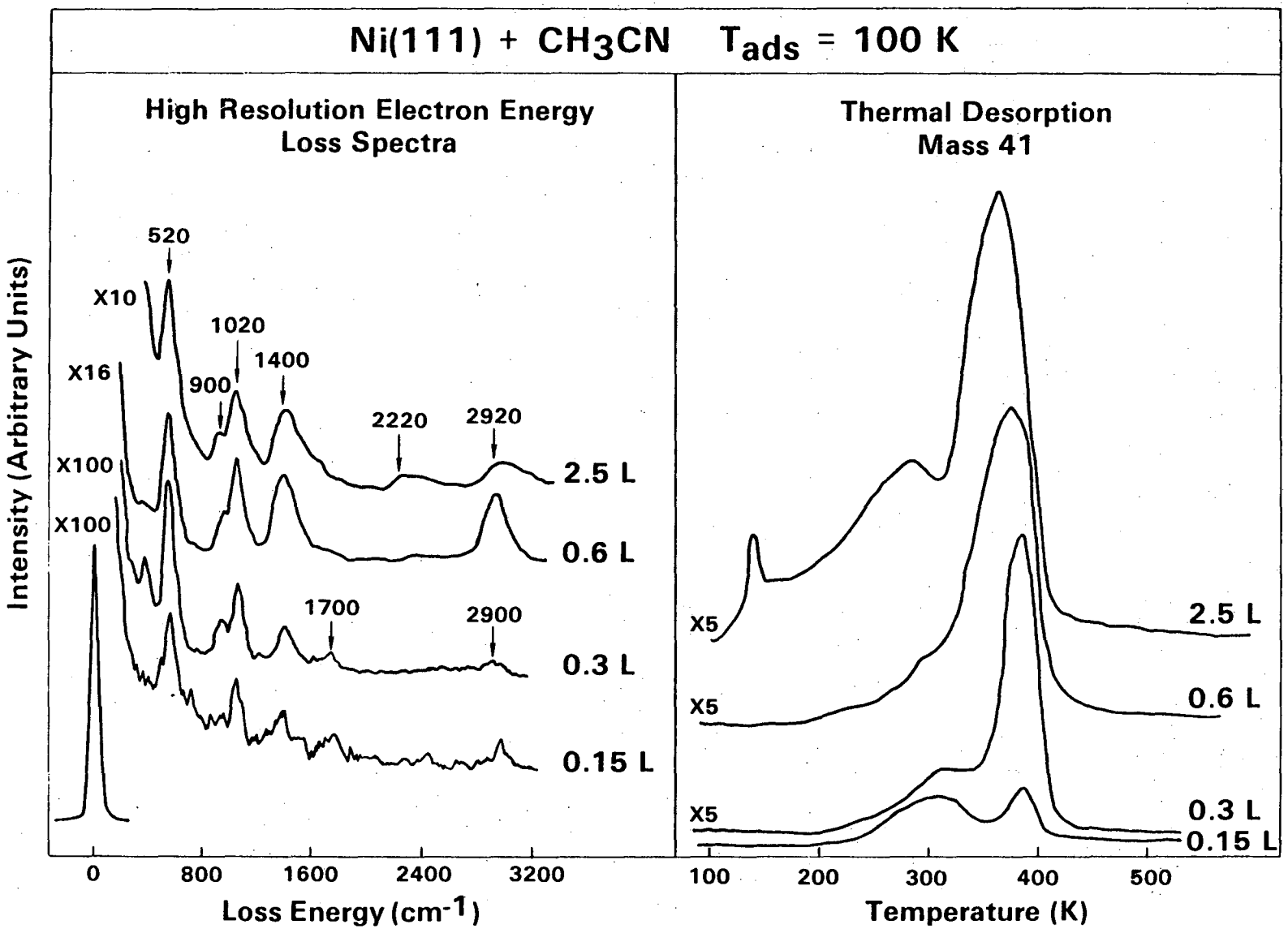

Figure 19.

XBL 817-10657

CH_3CN at 25°C followed by cooling to -170°C. Thus, the chemisorbed acetonitrile must undergo a reorganization of the surface structure.

The thermal desorption profile of mass 41 after CH_3CN adsorption on Ni(111)-C also contained three maxima with the peak temperatures for chemisorbed CH_3CN occurring at -20°C and 25°C, respectively, (Figure 20) significantly lower than for the clean Ni(111) surface. The coverage dependence for the manitudes of these two desorption peaks also differed from the Ni(111) case in that the lower temperature peak dominated the desorption spectrum at high coverages. As in the Ni(111) case, both chemisorbed desorption peaks were observed following adsorption of CH_3CN on the Ni(111)-C surface at 25°C and subsequent cooling to -170°C. Again, this is attributed to a reorganization of the CH_3CN chemisorbed layer.

The high resolution electron energy loss spectra of CH_3CN adsorbed at -170°C on Ni(111) and Ni(111)-C are shown as a function of coverage in Figures 19 and 21, respectively. The primary frequencies are summarized in Table 2 with the corresponding frequencies and assignments for gas phase acetonitrile. The key region was in the frequency range of 1500-2200 $cm.^{-1}$ where the CN stretching loss is expected. The loss observed at 2220-2240 $cm.^{-1}$ on both Ni(111) and Ni(111)-C at high CH_3CN coverages is assigned to the unperturbed CH Stretch in condensed CH_3CN; this may be compared to a frequency of 2252 $cm.^{-1}$ reported for solid CH_3CN.[45] At low coverages on the Ni(111) surface, the loss assigned as the CN stretch of chemisorbed CH_3CN was observed in the frequency range of 1680-1700 $cm.^{-1}$ (Figure 19). This transition was also evident after annealing the adsorbed multilayer at 25°C and is extremely low in relative intensity compared to other features in the spectrum as shown in Figure 22.

Figure 20. Shown in the figure are the spectra for CH_3CN (41 amu), H_2 (2 amu) and HCN (27 amu) obtained from thermal desorption of a multilayer of acetonitrile adsorbed on a carbided Ni(111) surface.

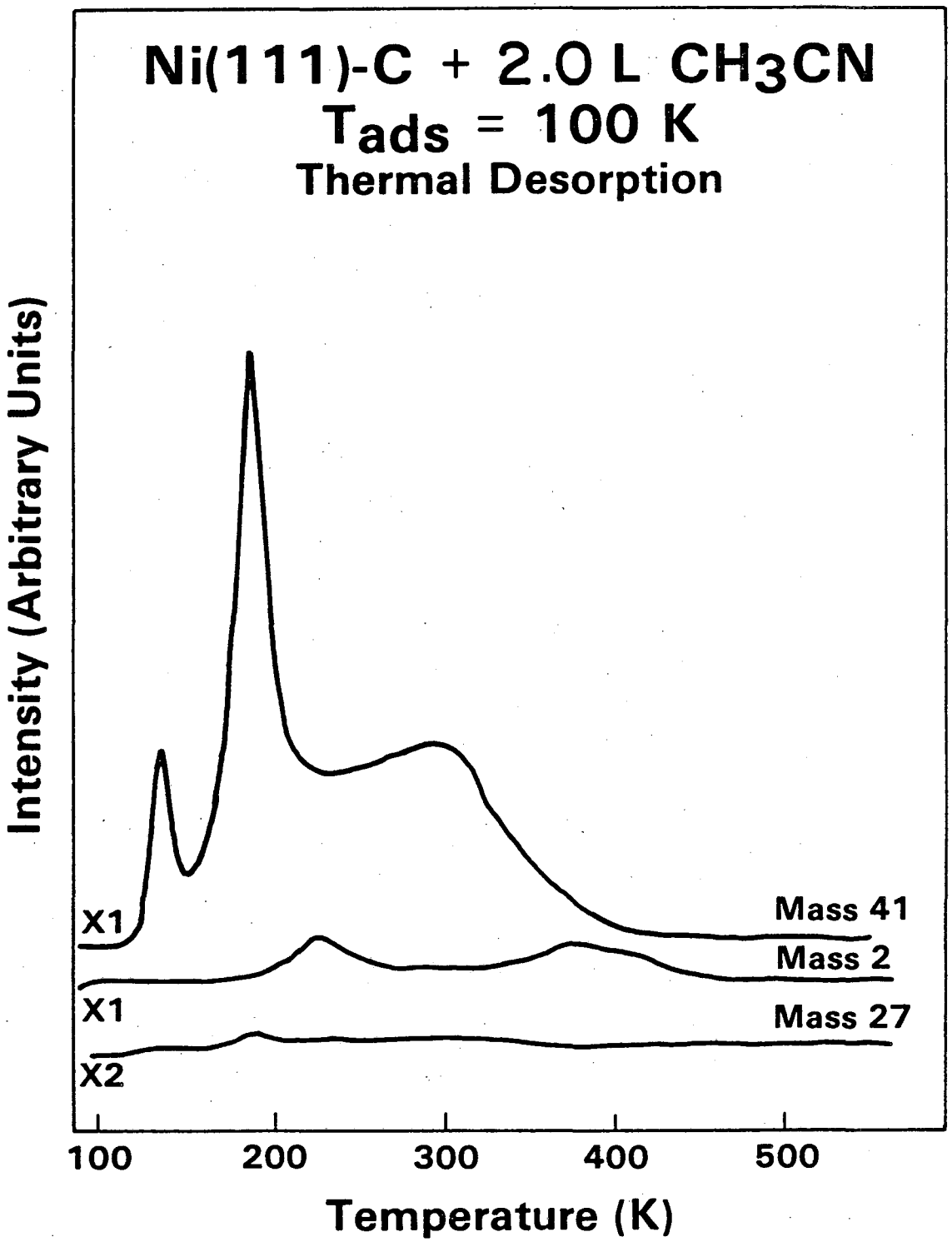

Figure 20.

XBL 815-9477

Figure 21. Vibrational spectra of CH_3CN adsorbed on Ni(111)-C and the corresponding thermal desorption spectra of molecular acetonitrile are shown in this figure as a function of coverage.

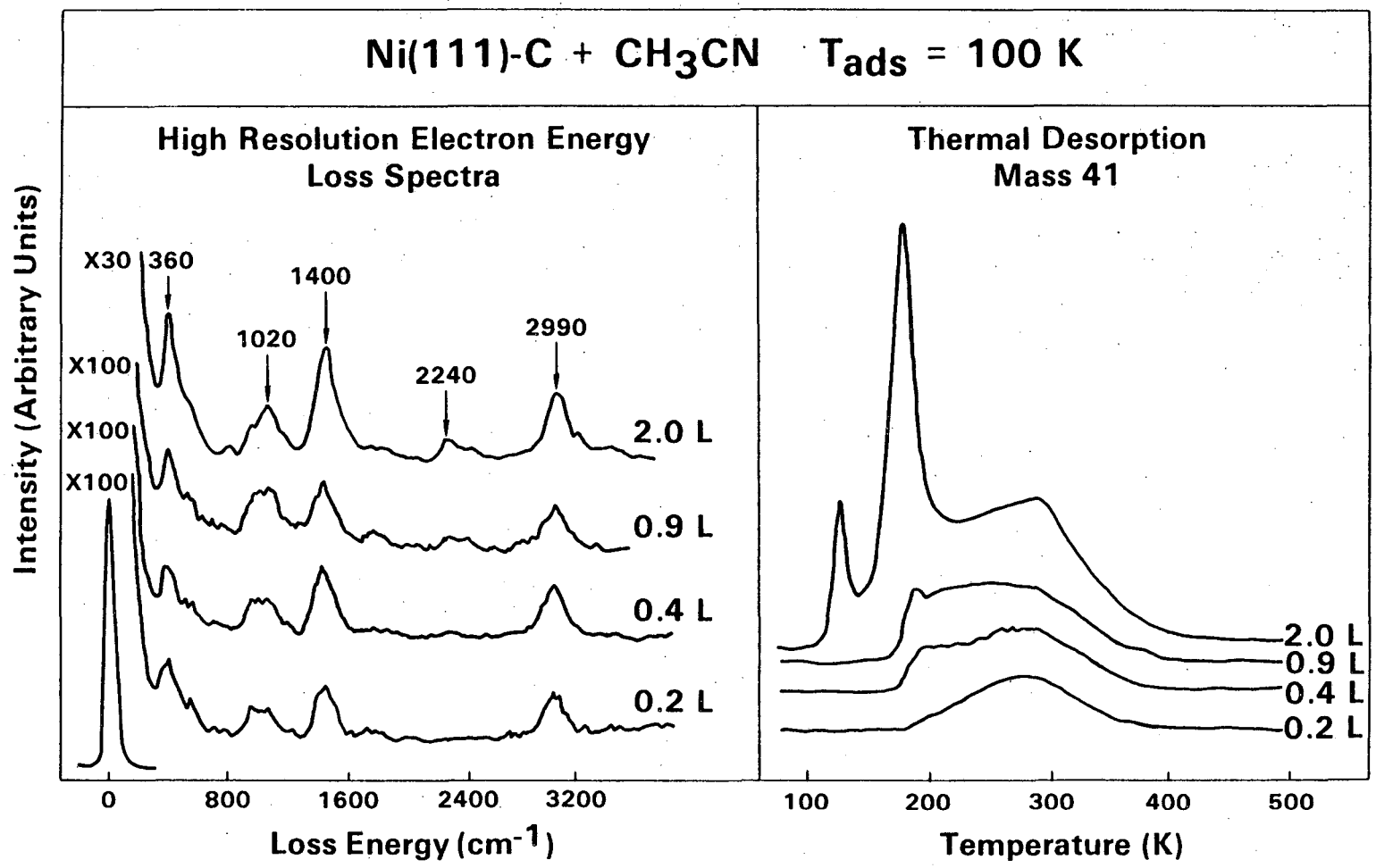

Figure 21.

XBL 817-10656

TABLE 2

Vibrational Data For CH_3CN

Ni (111)		Ni (111)-C		Gas Phase[44]	
Low Coverage ($cm.^{-1}$)	Annealed ($cm.^{-1}$)	Low Coverage ($cm.^{-1}$)	Annealed ($cm.^{-1}$)	($cm.^{-1}$)	Assignment
2900	2910	2990	2990	2954	ν(C-H)
1680-1700	1680	1800	1800	2267	ν(C-N)
1400	1400	1400	1400	1389	δ(HCH),δ(HCC)
--	900	980	980	920	ν(C-C)
1020	1020	1020	1020	1041	ρ(HCC)
520	520	--	--	--	see text
--	--	--	--	360	δ(NCC)

Figure 22. Depicted on the left in this figure are the high resolution electron energy loss data obtained from annealing a multilayer of acetonitrile adsorbed on a clean Ni(111) surface at -130°C and 25°C. The annealing temperatures are indicated in the 41 amu thermal desorption spectrum on the right. All energy loss data were collected with the crystal temperature maintained at -170°C, an incident beam energy of 2 eV and a resolution of 10 meV (80 $cm.^{-1}$).

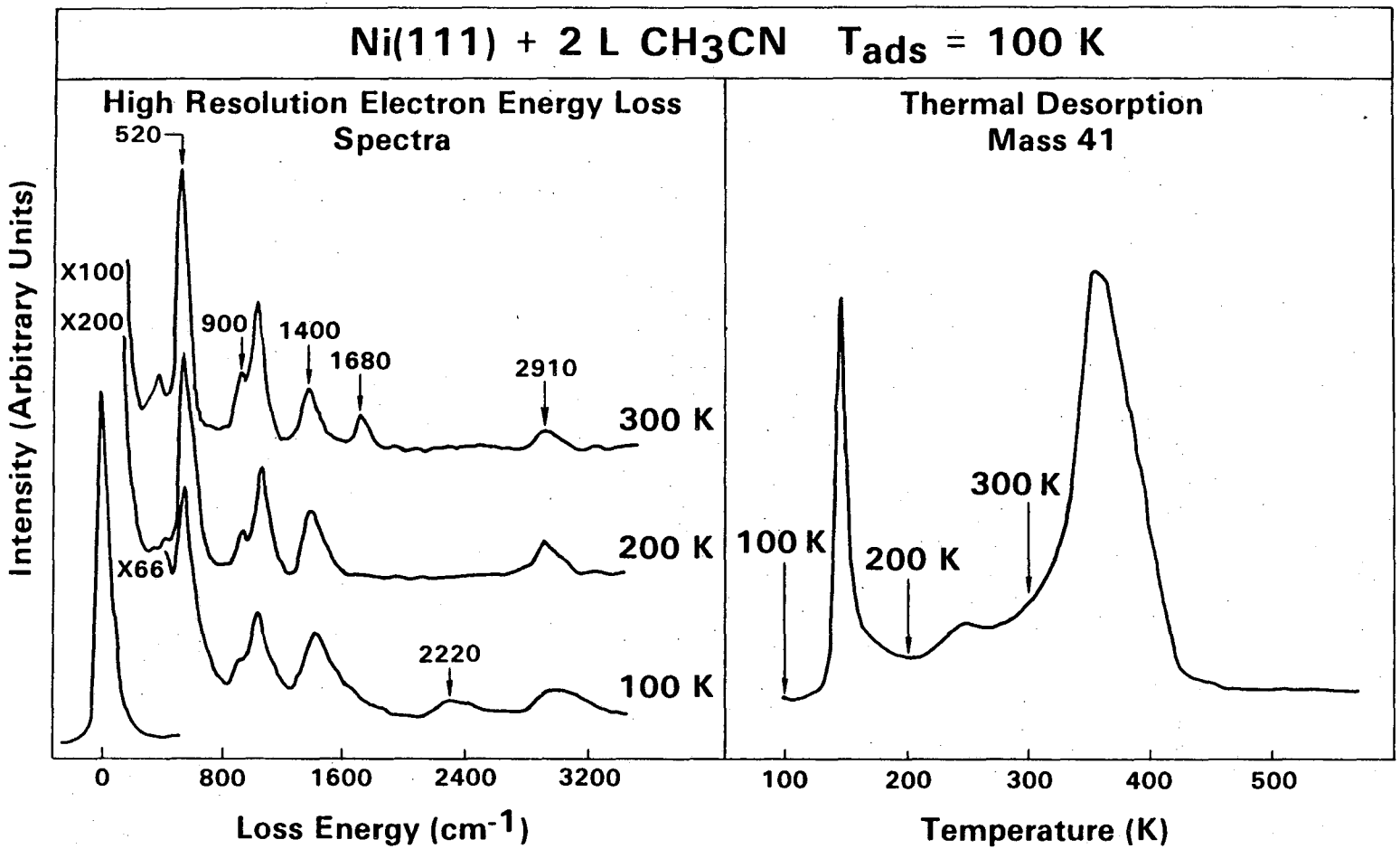

Figure 22.

XBL 817-10655

The most intense feature in the vibrational spectrum of CH_3CN adsorbed on Ni(111) is observed at 520 cm.$^{-1}$ This loss does not have a corresponding vibration in the solid acetonitrile spectrum. As shown in Figure 22, the 520 cm.$^{-1}$ loss grows in relative intensity upon annealing of the acetonitrile multilayer, i.e. upon desorption of condensed CH_3CN. Thus, the loss must be associated with chemisorbed acetonitrile and is tentatively assigned as either a Ni-N vibration or an asymmetric CCN bending mode perturbed by chemisorption to the nickel surface.

On the carbided Ni(111) surface, a slight shoulder at 1800 cm.$^{-1}$ is assigned to the CN stretch in chemisorbed acetonitrile. This is an extremely weak feature, present in spectra obtained at low CH_3CN coverages and subsequent to annealing the multilayer. (Figures 21 and 23). The 520 cm.$^{-1}$ loss is not present in the vibrational spectrum of CH_3CN adsorbed on a Ni(111)-C surface.

Comparison was made between the vibrational spectra obtained as a function of annealing temperature (Figures 22 and 23) and those obtained as a function of acetonitrile coverage (Figures 19 and 20); very little difference was noted for both the Ni(111) and Ni(111)-C surfaces. The appearance of the weak band in the range of 2220-2240 cm.$^{-1}$ can be correlated with sublimation of the condensed multilayer of CH_3CN. However, the two higher temperature desorption peaks could not be correlated with specific chemisorption states in the vibrational spectra. Again, this is suggestive of a reorganization of the CH_3CN overlayer upon cooling. Thus, it is likely that the vibrational data obtained at -170°C do not correspond to the surface species studied at temperatures above 25°C.

The frequency of the CN stretch of coordinated CH_3CN yields

Figure 23. A multilayer of acetonitrile condensed on a carbided Ni(111) surface at -170°C was annealed successively at -120°C, -30°C and 25°C and high resolution electron energy loss spectra presented on the left in the figure were obtained following annealing at each temperature. On the right, the annealing temperatures are indicated in the thermal desorption profile of molecular CH_3CN.

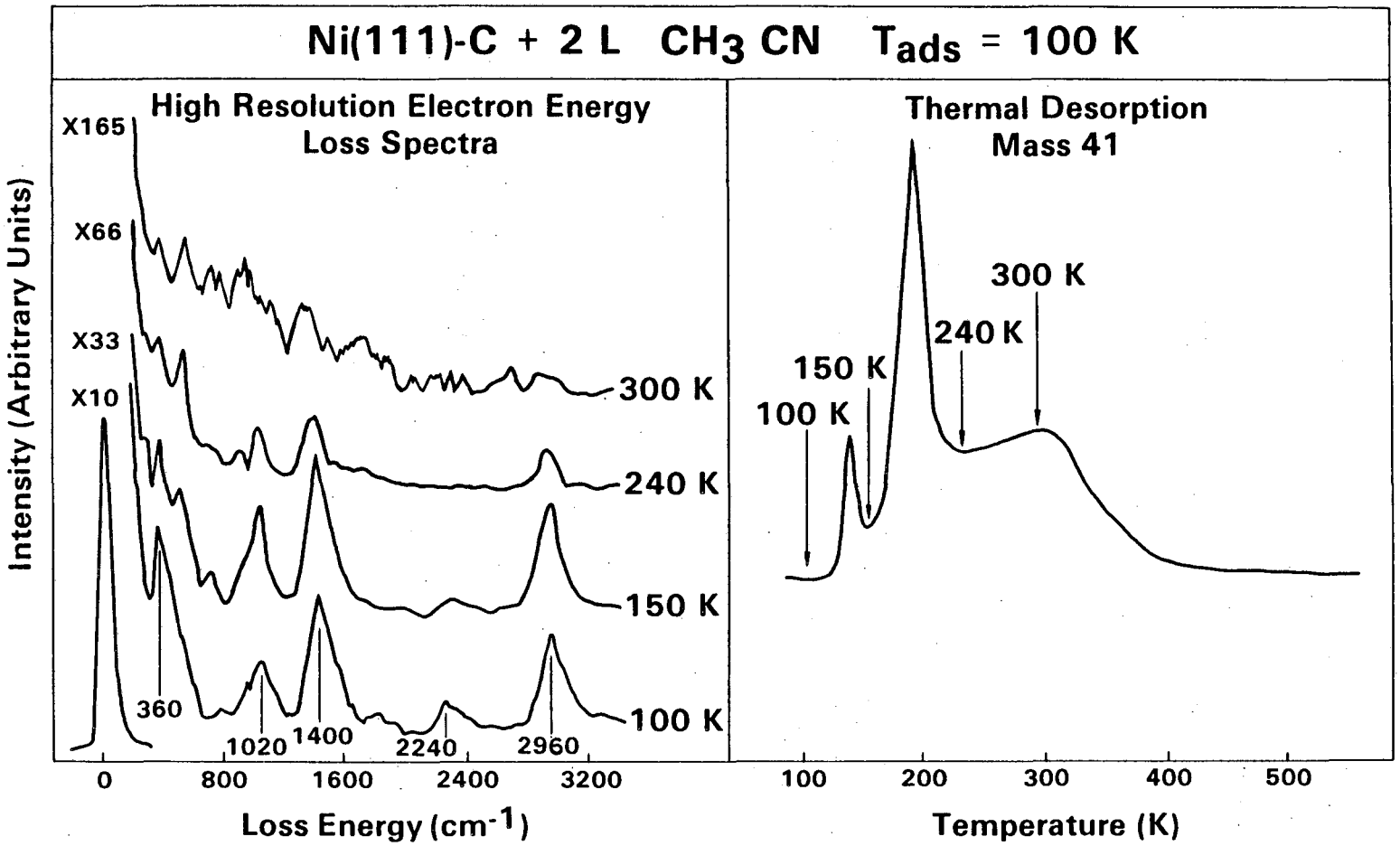

Figure 23.

XBL 815-9475

information about its structure in organometallic compounds. In the case of end on bonding, the CN stretching frequency is lowered depending on the amount of electronic back donation from the metal to the ligand π^* orbital, analogously to CO.[46] There are also examples of cluster compounds in which both the carbon and nitrogen atoms of the cyano group of the coordinated CH_3CN interact with metal centers.[47] Based on analogy to the cluster compounds, the CN stretching frequency would be expected to be in the range of 1500-1600 $cm.^{-1}$ for bonding to both the C and N, 1700-1800 $cm.^{-1}$ for bridge bonding and 2000-2100 $cm.^{-1}$ for acetonitrile bound atop a single metal center.

The frequency range of 1680-1700 $cm.^{-1}$ observed for CH_3CN adsorbed on Ni(111) at -170°C may be assigned to either a simple end-on bridging or structure or bonding via both the carbon and nitrogen atoms of the cyano group. On the basis of the dipole selection rule,[48] the low intensity of the CN stretch would also suggest a small dynamic dipole moment perpendicular to the metal surface. This comparison suggests a bonding configuration in which the CN bond vector was essentially parallel to the nickel plane. However, the intensity of the CN stretch in acetonitrile coordinated to metal atoms is generally low.[49] As pointed out previously, the (2x2) unit cell observed in low energy electron diffraction studies does not allow easily for packing of the CH_3CN molecule with the CN bond bector oriented parallel to the metal surface. The data obtained do not permit for a straightforward structural interpretation for chemisorbed CH_3CN on the Ni(111) surface; only bonding atop a single metal center can be unequivocally eliminated.

On the carbided nickel surface, the CN stretching frequency for

chemisorbed CH_3CN is increased to 1800 cm.$^{-1}$, in the range expected for end-on bridging of two or three metal centers via the nitrogen atom only. Again, bonding atop a single metal center can be ruled out based on the frequency of the CN stretch of 1800 cm.$^{-1}$ compared to an expected value of 2000 cm.$^{-1}$ The disappearance of the 520 cm.$^{-1}$ loss cannot be readily accounted for, although a mode involving Ni-N may be significantly affected by a change in surface electronic character induced by the carbide overlayer.

E. Methyl Isocyanide; Vibrational Studies on Ni(111) at -170°C

As in the case of acetonitrile, the thermal desorption spectrum observed following adsorption of a multilayer of CH_3NC at -170°C was qualitatively different than that obtained for adsorption at 25°C. (See Figure 24.) Two mass 41 desorption peaks were observed near -130°C and 20°C attributed to sublimation of condensed and desorption of chemisorbed methyl isocyanide, respectively. Two H_2 (mass 2) desorption peaks appeared at -10°C and 150°C indicating significant C-H bond scission below -10°C. Additionally, HCN was observed as a decomposition product desorbing at 260°C.

The extent of decomposition observed during a desorption experiment was reduced substantially when CH_3NC was adsorbed on a Ni(111)-C surface. At least, four mass 41 desorption peaks were present in the thermal desorption spectrum as shown in Figure 25. In addition to the -140°C and 20°C peaks, an unresolved double maximum was observed at 110 and 160°C. The H_2 desorption temperature decreased to 200°C and the amount of hydrogen produced during a desorption experiment decreased on the carbided nickel surface.

The energy loss data obtained for methyl isocyanide adsorbed on Ni(111) and Ni(111)-C adsorbed at -170°C are summarized in Table 3

Figure 24. The mass ion current as a function of temperature for 41 amu, 2 amu and 27 amu (HCN) following adsorption of a multilayer of methyl isocyanide on Ni(111) is illustrated here. The heating rate in this experiment was 10°C/sec.

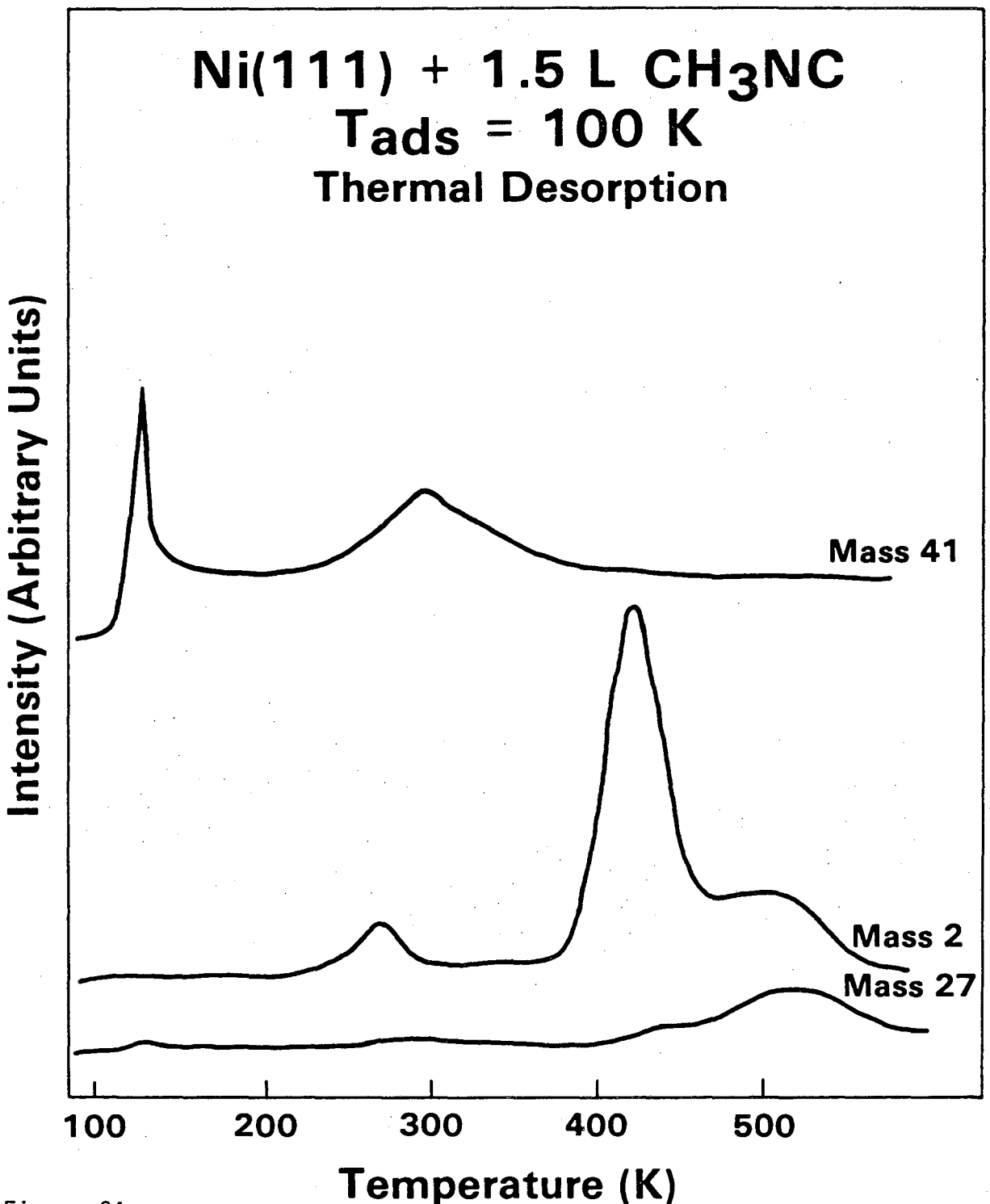

Figure 24.

XBL 817-10654

Figure 25. Thermal desorption of a multilayer of methyl isocyanide adsorbed on a Ni(111)-C surface yielded the spectra shown in the figure. Mass 41 corresponds to either CH_3NC or CH_3CN desorption; masses 2 and 27 correspond to desorption of the decomposition products, H_2 and HCN, respectively. The small peak in the 27 amu profile near 130K (-140°C) is derived from a fragment ion of CH_3NC.

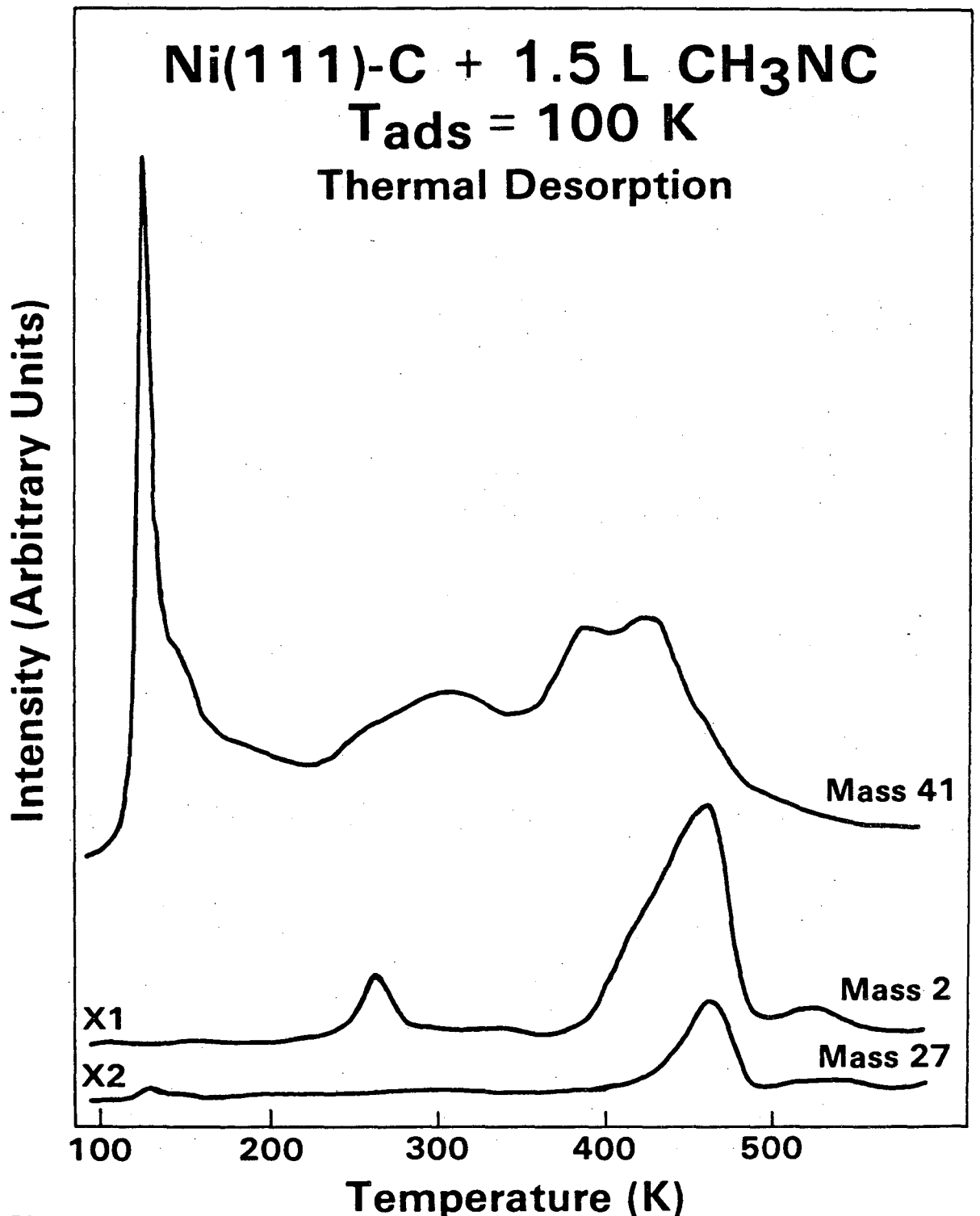

Figure 25.

XBL 815-9478

TABLE 3

Vibrational Data For CH_3NC

Ni (111)		Ni (111)-C		Gas Phase[44]	
Low Coverage ($cm.^{-1}$)	Annealed ($cm.^{-1}$)	Low Coverage ($cm.^{-1}$)	Annealed ($cm.^{-1}$)	($cm.^{-1}$)	Assignment
1120	1120	1120	1120	1130[50]	ρ(HCH)
1440	1480	1440	1420	1410,1460	δ(HCH)
1760	1700	1840,1940	1780,1900	2166	ν(N≡C)
2960	2860	2960	2960	2966	ν(HC)

with assignments based on gas phase infrared data. On the clean Ni(111) surface, the most intense feature in the spectrum was a loss in the frequency range of 1700-1760 cm.$^{-1}$, assigned as the CN stretch for chemisorbed methyl isocyanide. (Figures 26 and 27). At multilayer coverages, the unperturbed CN stretch for condensed CH_3NC occurred at 2160 cm.$^{-1}$

Two losses in the CN stretching region for CH_3NC adsorbed on Ni(111)-C were observed. At low coverages, the frequencies of the two losses were 1840 and 1940 cm.$^{-1}$ The higher frequency loss grew in relative intensity with increasing methyl isocyanide coverage. The results obtained for annealed overlayers of CH_3NC were qualitatively different than those obtained as a function of coverage; CN stretching frequencies decreased upon annealing at 340°C in contrast to the increase in frequency expected for a simple coverage dependence. This result is suggestive of an irreversible thermally induced transformation occurring on the surface. However, it is clear that the vibrational spectrum obtained after annealing the CH_3NC overlayer on the carbided surface is not the same as that observed for CH_3CN. If the isomerization is incomplete, the spectrum of the isomerized product may be obscured as there are not distinguishing features in the Ni(111)-C-CH_3CN spectrum. Alternatively, it may be concluded that the isomerization is reaction limited with desorption occurring immediately upon product formation.

Again, the CN stretching frequency can be used as a structural indicator for the chemisorbed CH_3NC analogously to CH_3CN. Adsorption atop a single metal atom can be eliminated for CH_3NC adsorbed on Ni(111) as the expected value for the CN stretch for atop bonding would be in the frequency range of 2000-2300 cm.$^{-1}$ By comparison

Figure 26. High resolution electron energy loss spectra were obtained following annealing of a multilayer of CH_3NC at -60°C and 25°C adsorbed on a Ni(111) surface and are depicted on the left. The location of the annealing temperatures with respect to the mass 41 desorption maxima are shown on the right in this figure.

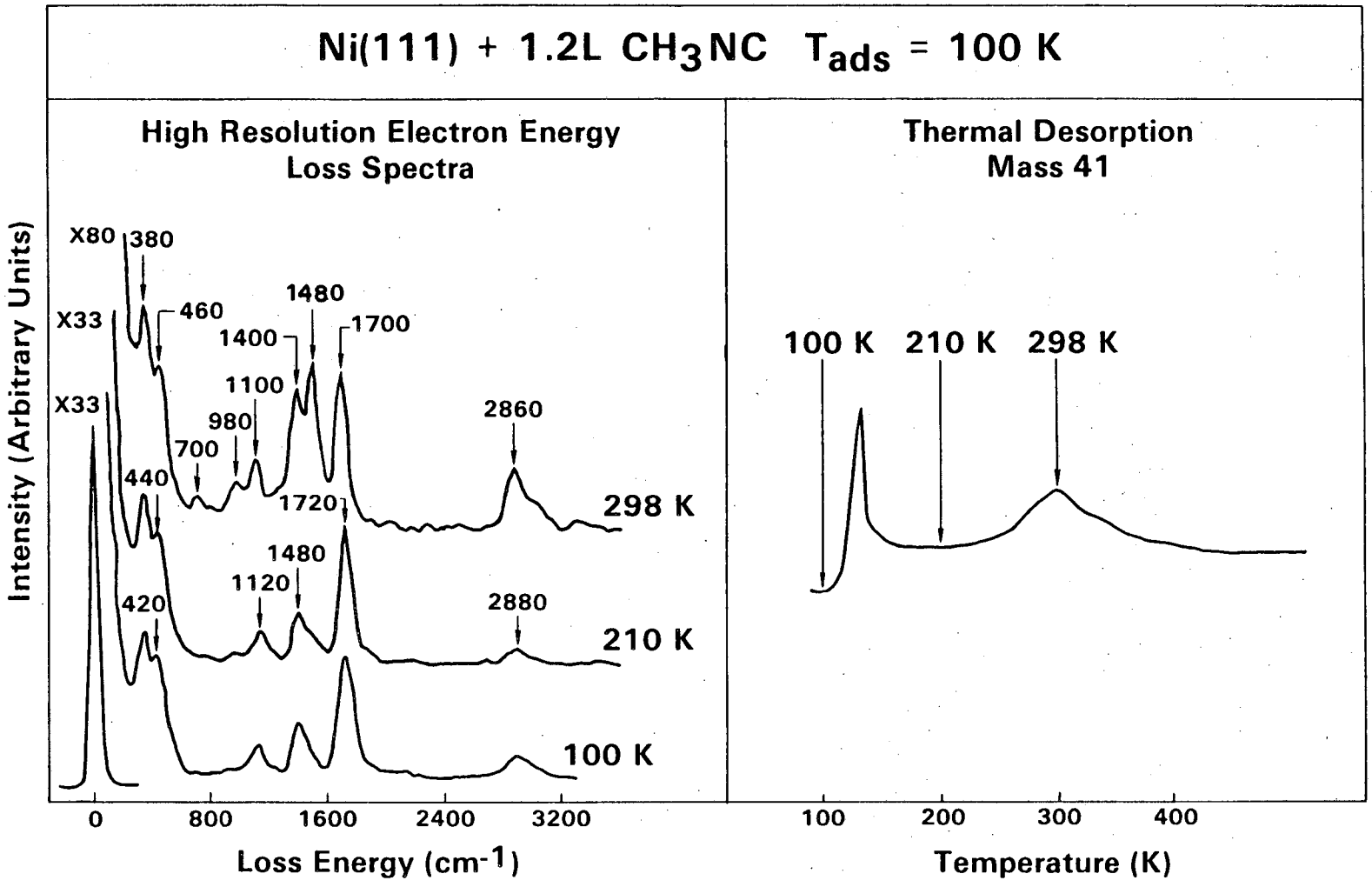

Figure 26.

XBL 815-9476

Figure 27. Vibrational spectra were obtained as a function of methyl isocyanide coverage on a clean Ni(111) surface and are presented in the left of the figure. The complimentary thermal desorption spectra of mass 41 (either CH_3NC or CH_3CN) are shown on the right. The resolution in the high resolution electron energy loss spectra varied as a function of coverage: for high CH_3NC coverages, the elastically scattered peak had a broad asymmetric tail giving rise to poor resolution (12 meV = 100 cm. $^{-1}$) and an asymmetry in the loss peak. This result was reproducible and thus must correspond to a property of the adsorbed multilayer. At lower coverages, the resolution was 10 meV (80 cm.$^{-1}$).

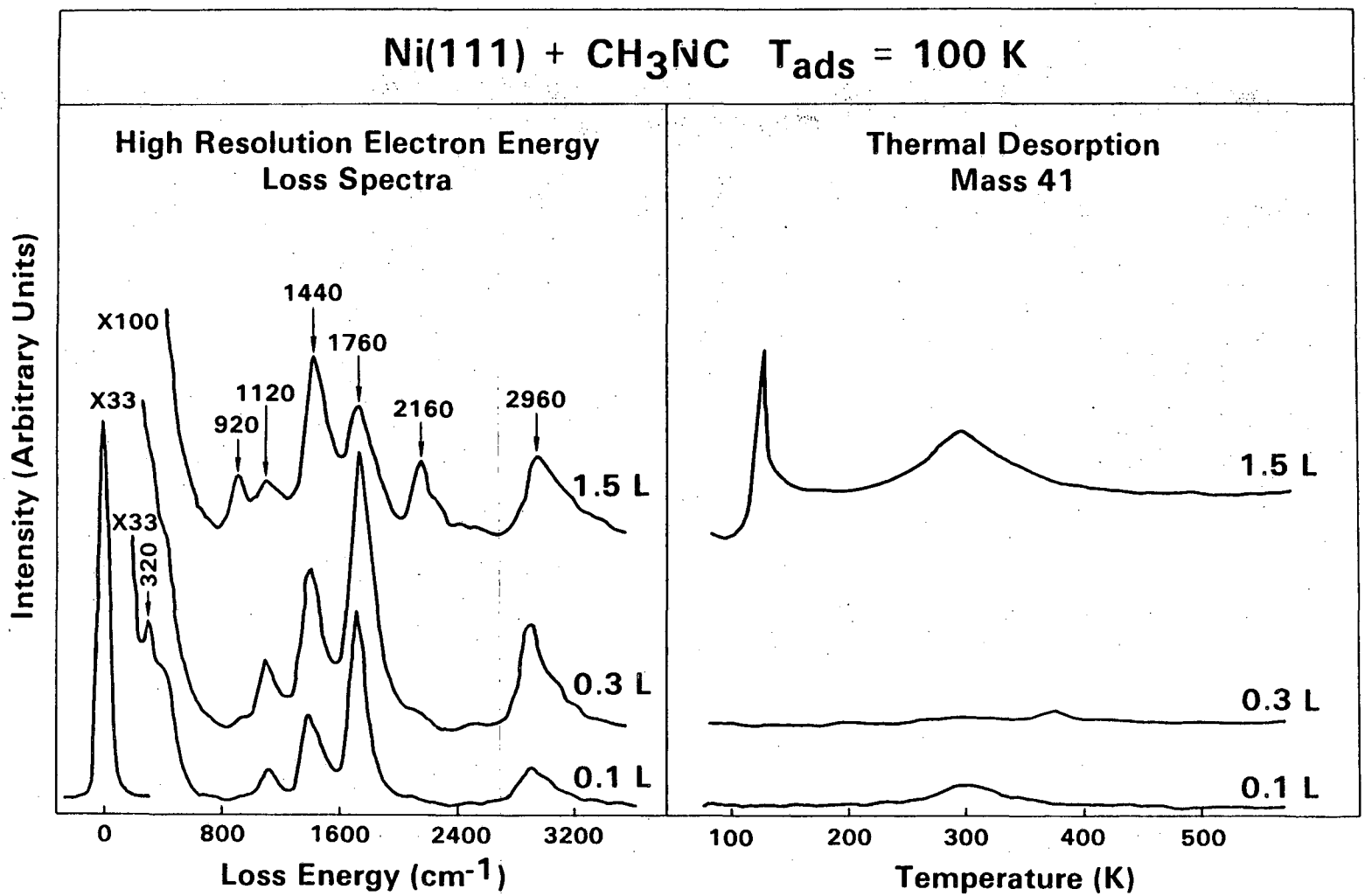

Figure 27.

XBL 817-10653

with values for the CN stretch in model compounds a bridging structure is most likely. End-on bridging is suggested by the large intensity of the CN stretching loss on the basis of the dipole selection rule. Specific chemisorption states cannot be readily correlated with the thermal desorption peaks by comparing the vibrational spectra for the annealed CH_3NC multilayer (Figure 26) with the coverage set (Figure 27).

The interpretation of the vibrational spectrum of CH_3NC adsorbed on Ni(111)-C is not straightforward. There are at least two chemisorption states on this surface as indicated by the two CN stretching frequencies at 1840 and 1940 $cm.^{-1}$ Both losses are very intense suggesting a bonding configuration in which the CN bond vector is directed close to the surface normal. The shift to higher frequency may be indicative of a site change or may reflect the increase in surface electronic denisty as a result of donation from the carbide to the metal. Again, specific vibrational states cannot be correlated with the different thermal desorption maxima by comparing the annealing and coverage sets of CH_3NC adsorbed on Ni(111)-C. (See figures 28 and 29). A more complete description of the two adsorption states will require further study.

2. Conclusions

A previously unreported catalytic reaction, the isomerization of CH_3NC to CH_3CN on carbided nickel surfaces, has been identified and studied using ultra-high vacuum surface techniques. Surface chemical studies have established that the adsorption of CH_3CN as molecular i.e. non-dissociative and fully reversible on both clean and carbided nickel surfaces with the exception of Ni(110). High resolution electron energy loss in conjunction with low energy electron diffrac-

Figure 28. A multilayer of methyl isocyanide adsorbed on Ni(111)-C was sequentially annealed at temperatures of -60°C, 25°C, 70°C and 100°C. The high resolution electron energy loss spectra obtained at -170°C subsequent to each annealing are shown on the left. The positions of the annealing temperatures in the mass 41 desorption profile are indicated on the right.

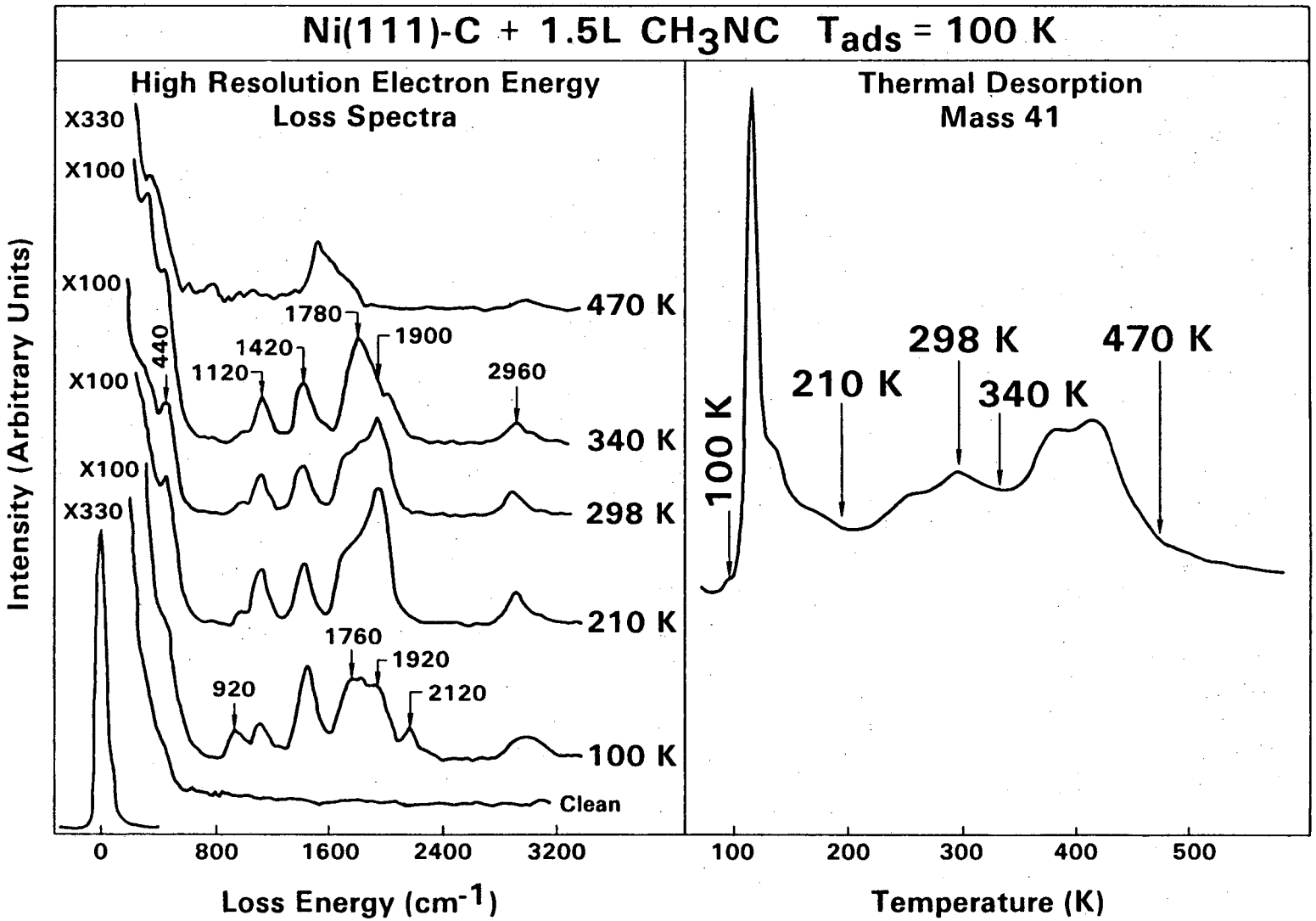

Figure 28.

XBL 817-10651

Figure 29. Vibrational data as a function of coverage for methyl isocyanide adsorbed on Ni(111)-C are presented in this figure on the left. As in the case of clean Ni(111), the elastically scattered peak was broad and asymmetric for high CH_3NC exposures, thus, the resolution varied between 10-12 meV (80-100 $cm.^{-1}$) as spectra were obtained from low to high CH_3NC exposures. On the right, the thermal desorption mass 41 profiles obtained subsequent to collection of the vibrational data are illustrated.

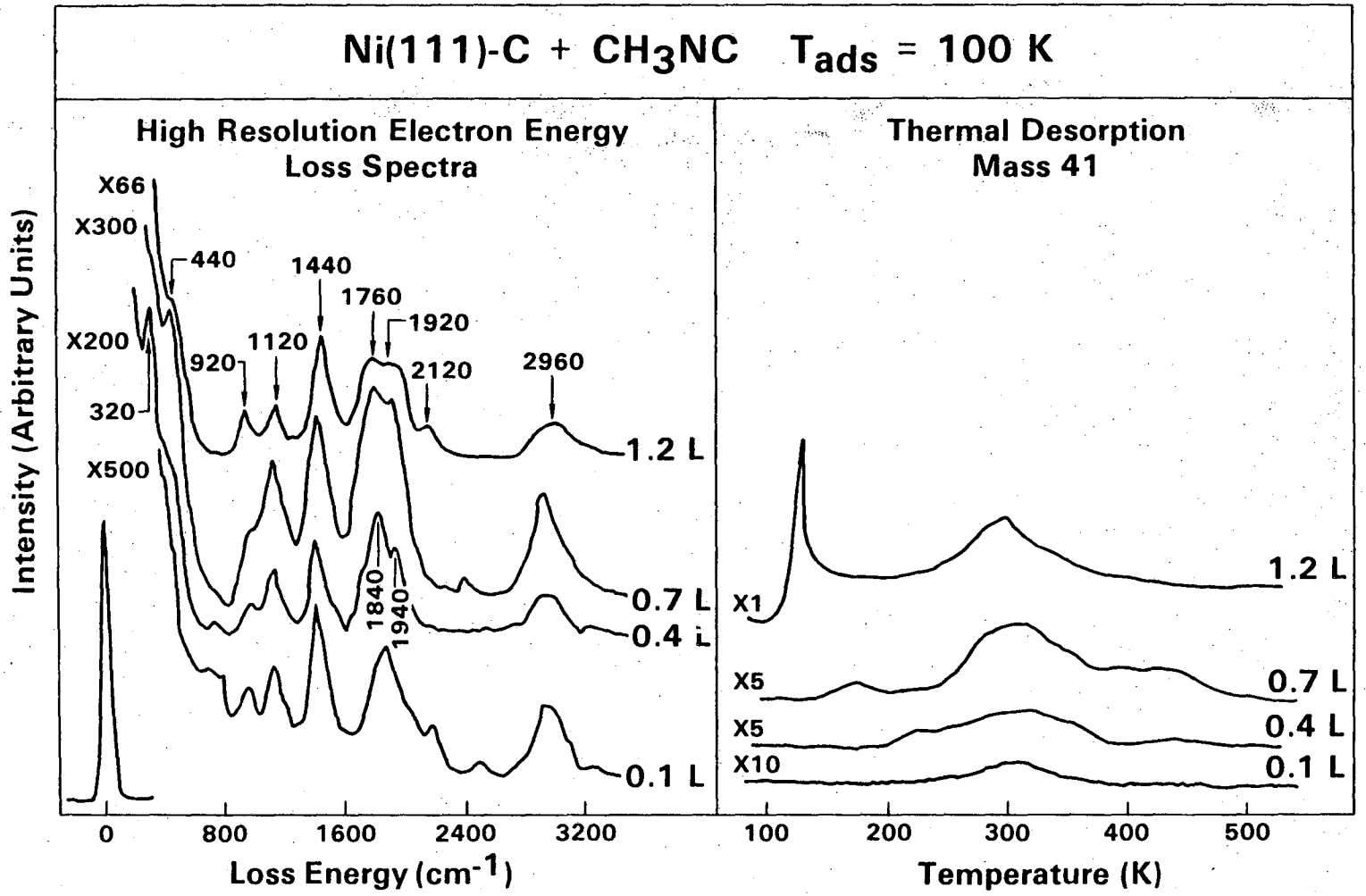

Figure 29.

XBL 817-10652

tion studies were supportive of a structure with CH_3CN bridging two or more metal centers via the nitrogen atom on Ni(111).

Methyl isocyanide was irreversibly adsorbed on clean nickel surfaces, but isomerized to the thermodynamically stable isomer, CH_3CN, on carbided nickel surfaces. Isotopic labelling studies established that the reaction mechanism was a fully intramolecular process; no isotopic scrambling was observed when a mixture of $CH_3N^{13}C$ and CD_3NC were isomerized and no ^{13}C-incorporation into the products was observed when the reaction was performed on a nickel surface with ^{13}C-labelled carbide. A CN stretching frequency in the range expected for a bridging isocyanide was observed in high resolution electron energy loss experiments performed at -170°C on Ni(111). Two CN stretching frequencies were found for CH_3NC adsorbed on Ni(111)-C at 170°C. The conversion of CH_3NC to CH_3CN on the surface was not observed using high resolution electron energy loss spectroscopy as of a function of annealing temperature. This may be due to the lack of distinguishing features in the CH_3CN spectrum or the isomerization may be reaction limited. The role of the surface carbide is still not well understood. The results described herein suggest that the carbide increases the surface electron density of the metal surface, thus favoring isomerization vs. dehydrogenation.

VII. APPENDIX

In this appendix, a collection of preliminary studies of pyridine, acetylene, ethylene and HCN adsorbed on nickel surfaces at 25°C are presented. Thermal desorption and chemical displacement reactions were the techniques used for these studies. Only experimental results will be presented with minimal interpretation. The data sets are incomplete and are presented for reference for future research.

1. Pyridine

The adsorption of pyridine has been studied on the three low Miller index surfaces, Ni(111), Ni(110) and Ni(100). In all cases, there was no significant thermal desorption of the intact pyridine molecule; only hydrogen molecule was desorbed with carbon and nitrogen remaining on the nickel surface. No displacement of intact pyridine was effected at 25°C by $P(CH_3)_3$ or CO. Thermal decomposition of perdeuteropyridine yielded a broad D_2 peak near 190°C from the Ni(110) surface and both D_2 and HD at 150°C from the Ni(111) surface. The D_2 profile obtained from the thermal decomposition of C_6D_5N adsorbed on Ni(100) was comprised of three maxima as shown in Figure 30. These three maxima are suggestive of sequential removal of hydrogen atoms on the ring with initial chemisorption via the nitrogen lone pair followed by facile abstraction of one of the hydrogen atoms. Thermal decomposition of the selectively labelled molecules, 1,5-^{2}d-pyridine 2,4-^{2}d-pyridine and 3-^{1}d-pyridine would resolve this issue.

2. Ethylene

The surface chemistry of ethylene on Ni(111) adsorbed at 25°C has been studied. Ethylene was irreversibly adsorbed; no thermal or desorption or chemical displacement in the temperature range of

Figure 30. Shown in this figure is the D_2 profile obtained following thermal decomposition of perdeuteropyridine adsorbed on Ni(100) at 25°C. The approximate exposure was 0.8 L. and the heating rate 20°C/sec.

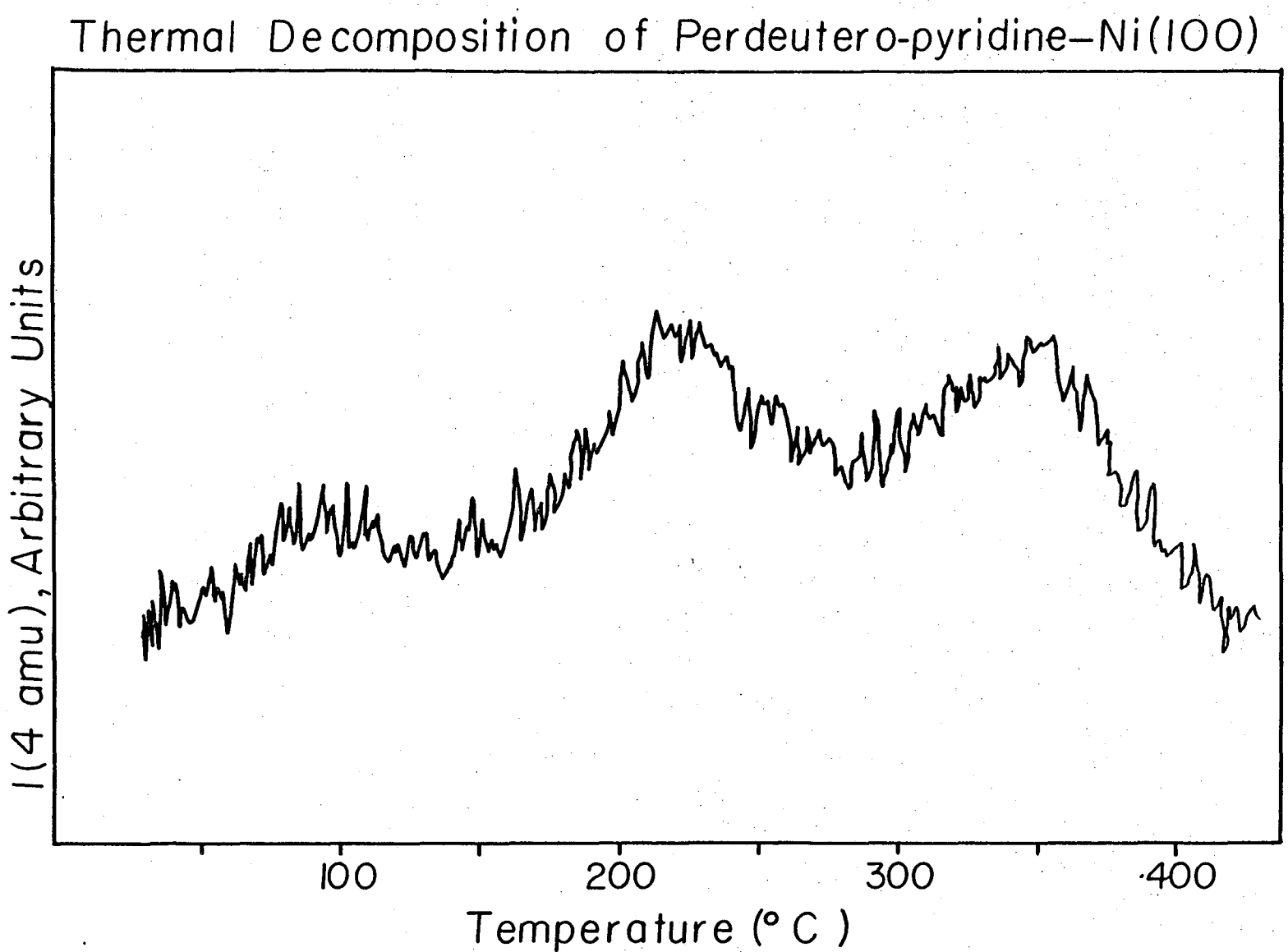

Figure 30.

XBL 817-10650

25-50°C of the intact molecule was detected. Trimethylphosphine, CO, benzene, cyanogen and methyl isocyanide were used in the attempted displacements. Thermal decomposition of C_2D_4 adsorbed on Ni(111) at 25°C yielded a double maximum for both HD and D_2 with the two desorption maxima located at 90 and 120°C. The sticking coefficient of ethylene was relatively low in comparison to acetylene, benzene or CO. Some degree of thermal reversibility may be observed if the desorption experiments were performed at higher coverages.

3. Acetylene

Acetylene, like ethylene, was irreversibly adsorbed on the Ni(111) surface following adsorption at 25°C. No detectable displacement could be effected by benzene, $P(CH_3)_3$, CO or CH_3NC. Thermal decomposition of C_2D_2 yielded only HD and D_2 with a peak temperature of 170°C with a significant amount of carbon remaining on the nickel surface.

VIII. ACKNOWLEDGEMENTS

I wish to thank and acknowledge Dr. Daniel A. Scherson for his love, encouragement, help and unwaivering confidence in me throughout my graduate career, Prof. Earl Muetterties for his helpful insight and for the rich and stimulating scientific environment that he provided, Dr. Judith Stein for synthesizing many of the organic reagents used, giving advice in the lab, for caring for Arturo while I was away and for general moral support, and Min-Chi Tsai for her collaboration in the lab and her friendship. Additionally, I wish to especially thank the superb support staff at Lawrence Berkeley Laboratories, in particular Glen Baum, Weyland Wong, Jim Severns, Lee Johnson, Keith Franck, without whom none of the experiments would have been possible, and Mr. Gary Mitchell for his guidance and advice in performing the high resolution electron energy loss studies at General Motors Research Laboratories. I wish to thank Ihsan for his love, humorous insight and for enriching my personal life. I thank and acknowledge the Dean of the Graduate Division and General Motors Research Laboratories for support of the vibrational studies, Gabor A. Somorjai and Alexis T. Bell, my thesis committee, and Sule Ozturkmen for her contribution to my degree, typing this thesis.

This work was supported by the Director, Office of Energy Research, Office of Basic Energy Sciences, Chemical Sciences Division of the U.S. Department of Energy under Contract Number W-7405-ENG-48.

IX. REFERENCES AND NOTES

1. G. A. Somorjai, Chemistry in Two Dimensions Surfaces, Cornell University Press, Ithaca (1981).
2. R. B. Moyes and P. B. Wells, Adv. in Cat., 23 (1973) 121 and references therein.
3. J. H. Sinfelt, Adv. in Cat. 23 (1973) 91.
4. G. Ertl and J. Kuppers, Low Energy Electron Diffraction and Surface Chemistry, Verlag Chemie (1974) 367.
5. See for example, J. E. Demuth, Surface Science 80 (1979) 367.
6. S. Y. Tong, C. H. Li and D. L. Mills, Phys. Rev. Let., 44 (6) (1980) 407.
7. E. L. Muetterties, T. N. Rhodin, Elliot Band, C. F. Brucker and W. R. Pretzer, Chem. Reviews 79 (2) (1979) 91.
8. a. C. M. Chan, R. Aris and W. H. Weinberg, Appl. Surface Science, 1 (1978) 360.

   b. C. M. Chan and W. H. Weinberg, Appl. Surface Science, 1 (1978) 377.
9. J. L. Falconer and R. J. Madix, Surface Science 48 (1975) 393.
10. F. Albert Cotton and Geoffrey Wilkinson, Advanced Inorganic Chemistry, 3rd ed. Interscience Publishers, John Wiley and Sons (1972) 658-670.
11. J. C. Hemminger, E. L. Muetterties and G. A. Somorjai, J. Am. Chem. Soc. 101 (1979) 62.
12. C. M. Friend and E. L. Muetterties, J. Am. Chem. Soc., 103 (1981) 773.
13. Jack Halpern, Adv. Chem. Ser., No. 70, 1-24 (American Chemical Society, Washington, D.C., 1968.)

14. C. J. Smitthels, Metals Reference Book, vol. 1, 3rd ed., Butterworths, Washington, D.C. (1962) 226.

15. Inorg. Synth. 9 (1967) 59.

16. Dr. Judith Stein synthesized the CH_3NC, CD_3NC, $CH_3N^{13}C$ and $P(CH_3)_3$ used in the studies described in the thesis.

17. J. Casanova, R. Shuster and N. Werner, J. Chem. Soc. (1963) 4280.

18. M. Gautier, Ann. Chim. Phys. 27 (1869) 103.

19. B. A. Sexton, J. Am. Vac. Soc. 16 (4) (1979) 1033.

20. J. C. Bertolini and B. Tardy, Surface Science 102 (1) (1981) 131.

21. T. V. Harris, J. W. Rathke and E. L. Muetterties, J. Amer. Chem. Soc. 100 (1978) 6966.

22. Further evidence suggesting a change in the nickel surface chemistry induced by phosphorous impurities is the thermal desorption behavior of $c\text{-}C_6H_{10}$ on Ni(110). No intact cyclohexene was thermally desorbed from the clean surface. However, a significant amount of $c\text{-}C_6H_{10}$ was thermally desorbed near 100°C upon coadsorption with $P(CH_3)_3$ at 25°C.

23. The mechanism of the displacement reaction is not understood, therefore, no explanation can be proffered to account for the incomplete displacement of benzene by methyl isocyanide. Attempts to force the displacement to completion by using larger CH_3NC exposures or increasing the temperature of the surface above 25°C were unsuccessful.

24. S. Lehwald, H. Ibach, J. E. Demuth, Surface Science 78 (1978) 577.

25. J. C. Bertolini, J. Rousseau, Surface Science 89 (1979) 467.

26. J. E. Demuth, D. E. Eastman, Phys. Rev. B 13 (4) (1976) 1523.

27. Displacement reactions were performed with the crystal face oriented along an axis 45° away from the line of sight of the

mass spectrometer ionizer. As a result, the mass ion signal of species desorbing from the surface was significantly decreased if a cosine-like distribution is assumed. Therefore, it is possible that displacement reaction products present in trace amounts were not detected.

28. HD was observed only in the high temperature peak when $CH_3C_6D_5$ was decomposed on the (111), 9(111)x(111) and 7(111)x(310) nickel surfaces. A small amount of HD was desorbed at higher temperatures for the decomposition of $CD_3C_6H_5$ on the above surfaces. Only a small amount of HD was desorbed at higher temperatures for the decomposition of $CD_3C_6H_5$ on Ni(100) with a maximum of 170°C. No HD was produced in the $CH_3C_6D_5$ Ni(100) case. These results are indicative of the overlap in the two decomposition peaks allowing some free deuterium to remain on the surface and recombine with surface hydrogen at a temperature higher than the lower temperature desorption maximum.

29. No significant difference in the desorption maxima for H_2 compared to D_2 was observed.

30. E. Crawford and C. Kemball, Trans. Faraday Soc. 58 (1962) 2452, showed that H-D exchange between D_2 and alkyl benzenes on nickel films was faster with CH hydrogen atoms than with ring hydrogen atoms. For toluene, the ratio of $R_{CH_3}/R_{C_6H_5}$ was 13 at 0°C for unsintered Ni films. For sintered films, the ratio of initial exchange was 230 at 120°C.

31. J. E. Demuth, H. Ibach and S. Lehwald, Phys. Rev. Lett. 40 (15) (1978) 1044.

32. The relative sticking coefficients were estimated by comparing the Auger C(272 eV)/Ni(61 eV) ratio following the same exposures

of benzene and cyclohexene.

33. D. Wayne Goodmann, John T. Yates and T. E. Madey, Surface Science Lett. 93 (1980) L 135.

34. No significant reversible or irreversible C-H bond cleavage occurred for benzene itself on the low Miller index nickel surfaces. Thus, any C-H bond breaking and making observed would have to be attributed to a step in the dehydrogenation mechanism.

35. The relative sticking coefficient was estimated by integrating over all desorbed products (CH_3CN and H_2) and comparing the normalized total desorption from the clean and contaminated surfaces.

36. The extent of displacement was verified by two methods:
    a. Auger electron spectroscopy following displacement was used to probe for the presence of surface nitrogen.
    b. Thermal desorption subsequent to displacement of CD_3CN was used to probe for deuterium-containing products desorbing from the surface.

37. Carbon-hydrogen bonds are proposed to be activated via formation of C-H-Ni bridging interactions. If there were a significant degree of this bridging interaction for chemisorbed acetonitrile, dehydrogenation should compete effectively with molecular desorption.

38. J. Kouba and E. L. Muetterties, unpublished data.

39. The actual mixture contained CH_3NC, $CH_3N^{13}C$ and CD_3NC. The relative intensities of the parent ions of these molecules was the same for the initial mixture and the thermally desorbed gases indicative of no isotopic mixing.

40. a. J. P. Biberian and G. A. Somorjai, Appl. Surf. Sci. 2 (1979) 352.

b. In our experiments, the presence of nitrogen on the surface may have made the carbon coverage estimates slightly high.

41. V. W. Day, R. O. Day, R. S. Kristoff, F. J. Hirsekorn and E. L. Muetterties, J. Am. Chem. Soc., 97 (1975) 2571.

42. Control experiments using the reactor without the nickel catalyst did not yield any gas phase isomerization until temperatures near 250°C.

43. Carbon is a pervasive impurity for all nickel surfaces. Additionally, the initial CH_3NC molecules that interacted with the catalyst persumably decomposed leaving residual carbon and nitrogen on the surface.

44. Y. Hase and O. Sala, An. Acad. Bras. Cienc., 45 (1973) 381.

45. R. J. Jacobsen and Y. Mikawa, Applied Optics (1) (1970) 17.

46. Tom Ziegler and Arvi Rauk, Inorg. Chem. 18 (17) (1979) 1755.

47. M. A. Andrews, C. B. Knobler and H. D. Kaesz, J. Am. Chem. Soc. 101 (1979) 7260.

48. a. E. Evans and D. L. Mills, Phys. Rev. B 5 (10) (1972) 4126.

b. H. Ibach, Surface Science 66 (1977) 56.

49. The oscillator strength of the CN couple is weak for gaseous acetonitrile compared to other molecules with a CN group. Additionally, the CN stretch for acetonitrile bound to transition metals is typically low in intensity. For example, the CN stretch for cis-$MoCl_4(NCCH_3)_2$ in solid or solution infrared was undetectable.

50. Teresa B. Freedman and Eugene R. Nixon, Spectrochim. Acta 28A (1972) 1375.

This report was done with support from the Department of Energy. Any conclusions or opinions expressed in this report represent solely those of the author(s) and not necessarily those of The Regents of the University of California, the Lawrence Berkeley Laboratory or the Department of Energy.

Reference to a company or product name does not imply approval or recommendation of the product by the University of California or the U.S. Department of Energy to the exclusion of others that may be suitable.

TECHNICAL INFORMATION DEPARTMENT
LAWRENCE BERKELEY LABORATORY
UNIVERSITY OF CALIFORNIA
BERKELEY, CALIFORNIA 94720